Annu. Rev. Astron. Astrophys. 2000. 38:573–611

MASS LOSS FROM COOL STARS: Impact on the Evolution of Stars and Stellar Populations

Lee Anne Willson
Department of Physics and Astronomy, Iowa State University;
e-mail: lwillson@iastate.edu

Key Words Stellar evolution, stellar winds, asymptotic giant stars, circumstellar dust, Mira variables

■ **Abstract** This review emphasizes the mass loss processes that affect the fates of single stars with initial masses between one and nine solar masses. Just one epoch of mass loss has been clearly demonstrated to be important for these stars; that is the episode that ends their evolution up the asymptotic giant branch. Quite a clear picture of this evolutionary stage is emerging from current studies. Mass loss rates increase precipitously as stars evolve toward greater luminosity and radius and decreased effective temperature. As a result, empirical relationships between mass loss rates and stellar parameters are determined mostly by selection effects and tell us which stars are losing mass rather than how stars lose mass. After detailed theoretical models are found to match observational constraints, the models may be used to extrapolate to populations not available for study nearby, such as young stars with low metallicity. The fates of stars are found to depend on both their initial masses and their initial metallicities; a larger proportion of low-metallicity stars should end up with core masses reaching the Chandrasekhar limit, giving rise to Type 1.5 supernovae, and the remnant white dwarfs of low-Z populations will be both fewer and more massive than those in Population I. There are also clear indications that some stars lose one to several tenths of a solar mass during the helium core flash, but neither models nor observations reveal any details of this process yet. The observational and theoretical bases for a variety of mass loss formulae in current use are also reviewed in this article, and the relations are compared in a series of figures.

INTRODUCTION

During the past two decades, enormous strides have been taken in the detection of outflows from stars, including the massive outflows that end the nuclear burning evolution of stars like the Sun. Considerable effort has gone into understanding these observations through a variety of theoretical models. In this review, I emphasize the study of mass loss processes and events that affect the post–main-sequence evolution of stars up to about 9 M_{Sun}, and determine their final remnant masses. In Population I, these stars ascend the asymptotic giant branch (AGB) and end their

lives as white dwarf stars. With less efficient mass loss, as is likely for Pop II or Pop III stars, a significant fraction of the 3–10 M_{Sun} stars will end up producing supernovae of Type 1.5, with largely unexplored consequences for the early chemical evolution of our galaxy.

A number of interesting reviews relevant to this topic have appeared over the years. In the first volume of *ARAA*, Weymann reviewed mass loss from stars (Weymann 1963). More recently, Holzer & Axford (1970) covered stellar wind theory, Kwok (1993) emphasized the transition from the AGB to PNE, and Weidemann (1990) discussed the relationship of initial mass to final mass in his review of white dwarfs. Dupree (1986) reviewed mass loss from cool stars in 1986, emphasizing spectroscopic signatures and solar-type winds, and Zuckerman (1980) reviewed envelopes around late-type giants. In another article in this volume, Kudritzki reviews mass loss from hot stars. Iben & Renzini (1983; Iben 1974) described single star evolution from the main sequence onward, including some effects of mass loss. Chiosi & Maeder (1986) reviewed massive star evolution with mass loss for this series, and Chiosi et al (1992) included discussion of mass loss in their article on the HR diagram. Recent conference proceedings of note include *Physical Processes in Red Giants* (Iben & Renzini 1981), *Late Stages of Stellar Evolution* (Kwok & Pottasch 1987), and *Asymptotic Giant Branch Stars* (Le Bertre et al 1999). *Mass Loss from Red Giants* (Morris & Zuckerman 1985) includes a number of excellent reviews that are still timely.

Interpreting observations of winds and measuring mass loss rates require an understanding of the nature of the flow and thus of the mechanisms that drive mass loss. Three types of winds that have received the most attention for cool stars are solar-type winds, dust-driven winds, and pulsation-initiated winds. These mechanisms are briefly reviewed in Section 1. In the development of evolutionary studies of stars and populations, if mass loss is taken into account at all, it has been done using empirical mass loss. The observational basis for these empirical formulae is discussed in Section 2, with consideration for both the mass loss rates derived from observations and the uncertainties in the other parameters of the mass-losing stars. In the final section, the mass loss epoch that ends the AGB stage of evolution is examined in detail, both because it is particularly important for the evolution of low-mass stars and because it is an example of how empirical mass loss laws can be interpreted in more than one way with very different consequences. From a careful mating of theoretical models with observational constraints it is possible to derive predictions for the mass loss history of populations not presently available for study, such as young, low-metallicity populations that were important when our galaxy was much younger.

The evolution of low- and intermediate-mass stars without mass loss is reviewed in many textbooks, and most authoritatively by Iben (1974; Iben & Renzini 1983); red giant branch development is described in detail by Sweigart & Gross (1978; also Sweigart et al 1990). Briefly, low-mass stars leave the main sequence and migrate

to the red giant branch (RGB) after core H exhaustion. They evolve up the RGB with hydrogen-burning shells around growing degenerate He cores. For those stars with $M < 2$–$3\ M_{Sun}$ (depending on composition), the RGB ends with a helium core flash, after which the star settles down to convert He to C in its core on the horizontal branch or in the red giant "clump." Slightly more massive stars loop to the left in the HRD during core He burning without such an abrupt beginning. After the He in the core has been converted to C and O, the core becomes degenerate, and shell-hydrogen burning recommences. The shell burning builds up a degenerate helium layer around the core; this layer "flashes" into renewed helium burning each time its mass reaches a critical value. Thus, H and He burning alternate as the star evolves up the asymptotic giant branch (AGB or thermally pulsing AGB). When the mass of the hydrogen-rich envelope becomes quite small—either because of conversion to He and C+O or because of mass loss—the star leaves the AGB, migrating toward hotter temperatures where it may spend some time as the central star of a planetary nebula before cooling as a white dwarf (e.g. Schönberner 1983). This general picture is well confirmed by observations, including period changes and the formation of discrete circumstellar shells consistent with variations expected during individual shell flashes (Wood & Zarro 1981; Sterken et al 1999; Olofsson et al 1990, 1996; Hashimoto et al 1998).

Mass loss determines several features of stellar populations that are important for interpreting a wide variety of observations. Mass loss determines the maximum luminosity achieved by AGB stars, the most luminous red stars in populations older than about 0.1 Gyr and younger than about 10 Gyr. Mass loss determines the mass spectrum of white dwarfs, and this in turn affects their cooling times. Mass loss determines the masses of the central stars of planetary nebulae, and this in turn determines the planetary nebula luminosity function. Mass loss determines the frequency of supernovae of type 1.5 and II, and possibly the masses of the progenitors of Type I supernovae, and this affects both the use of supernovae as probes of distant galaxy populations and distances and the chemical evolution of galaxies. Mass loss determines the maximum radius the star achieves, and thus the fates of any planets in orbit around it (LA Willson and GH Bowen 2000, in prep).

Direct observational constraints on mass loss from stars cover a limited range of populations. In our galaxy, we have young stars of high metallicity and old stars of low metallicity available to study. When our galaxy was young, however, the stars were young and of low metallicity. To understand the chemical evolution of our galaxy and the appearance of young populations of low Z outside our galaxy, we need to know the mass loss patterns of populations whose mass loss rates we cannot study directly. The solution to this apparent impasse is the same as the solution to the problem of determining the ages of stars: Rather than looking at individual objects and then trying to fit empirical relations to these for use in models, we should look at the evolution of populations of stars and fit these to theoretical models that have already been checked against cases that can be more directly observed.

1. ELEMENTS OF THE THEORY

Theoretical studies of red giant winds are examined in this section for (a) solar-type winds in the framework of stationary outflows, (b) stationary outflows involving dust, and (c) winds from pulsating stars. The conclusion is reached that at least the massive outflows of highly evolved giants must be attributed to pulsation, acting alone in some cases and providing the opportunity for dust to form in others.

1.1 Stationary Wind Theory

The hydrodynamic theory of stationary, supersonic stellar winds was developed in a classic series of papers by Parker (1960; 1961; 1963a,b; 1964a,b,c; 1965; 1966; 1969; see also Parker 1997 for a review of the history of the subject, and Weymann 1963 for a succinct summary). Such flows are governed by an equation of the form

$$1/v\ dv/dr = (2/r)[A(r) - B(r)]/\left(v^2 - {c_T}^2\right), \tag{1}$$

where ${c_T}^2 = P/\rho$. For a spherically symmetric, isothermal, thermally driven wind, $A = {c_T}^2 =$ constant and $B = {v_{esc}}^2/\ 4 = GM/2r$. A critical point, r_P, occurs where $A = B$. If v is less than c_T at r_P, then the flow decelerates beyond r_P. This solution requires pressure greatly exceeding typical interstellar values in most cases. A static atmosphere with T(r) declining more slowly than 1/r also requires unreasonably high pressure at infinity to contain it. If T is proportional to 1/r, then there is no critical point and the flow must remain subsonic; see Parker (1965) for more detailed discussion of these and related points. If v reaches c_T below r_P, then formally the acceleration becomes infinite, so such solutions are excluded. More physically, once $(1/v\ dv/dr)^{-1}$ becomes less than the gas mean free path (i.e. for a large Knudsen number), the hydrodynamic approximation breaks down, and the equations no longer apply. Oscillatory solutions around $v = c_T$ may then occur in real stars (GH Bowen, private communication), but they fall outside the theory of stationary flows.

If the outflow carries very little mass, then the mean free path is large, and the thermal velocity distribution is no longer isotropic and Maxwellian even below the critical point. In that case, the loss of mass occurs by evaporation from the "exosphere" rather than by hydrodynamic outflow. This tends to result in a slow sonic flow interior to the exosphere, along with the selective loss of light/fast particles from it, a situation frequently encountered in the context of planetary atmospheres (Chamberlain 1960, 1961, 1963).

Whether the flow is hydrodynamic or evaporative, the ratio $4{c_T}^2/{v_{esc}}^2 = 2H_s/r$ (where H_s is the static, isothermal scale height) appears as a critical parameter, and the flow may be said to originate from the region where $2H_s/r \sim 1$. For stars with atmospheres in radiative equilibrium, H_s/R^* ranges from $<10_{-4}$ for main sequence stars to $<10_{-2}$ for the most extreme giants, putting the critical point very far from the star. From this, we conclude that a stellar wind requires a driving

mechanism to heat the atmosphere, accelerate the flow, and/or reduce the effective gravity substantially.

Driving mechanisms that have been invoked and studied in the formalism of the steady wind theory include thermally driven winds (with various mechanisms providing the extra heating), winds where acoustic and/or Alfvén waves are invoked to deposit momentum and energy in the material, and winds driven by the momentum of starlight ("radiation pressure" driven winds). Although thermally driven winds remain the textbook example, they are probably rarely important in practice. As was pointed out by Holzer & MacGregor (1985), the radiative losses associated with the required hot coronal material would exceed the stellar luminosity in most cool stars. This fact should perhaps not come as a surprise, now that we have clear evidence from X-ray imaging that the solar wind flows from the (cool) coronal holes and the hot coronal material is trapped in the closed magnetic loops.

Winds from hot stars are driven by the absorption and scattering of resonance line photons in the UV. Winds from cool stars could be similarly accelerated by radiation pressure acting through absorption or scattering in molecular bands, in the continuum (for a chromosphere or corona), or from dust (of which more later). The effects on cool star atmospheres and winds of radiation pressure acting in molecular lines have been investigated by Jørgensen & Johnson (1992), Maciel (1976), and Elitzur et al (1989). Unless red giants are much cooler and lower-gravity than now appears likely, this mechanism is probably important only for the effect it has on the scale height deep in the atmosphere; the wind is enhanced but not driven by radiation pressure on molecules (Höfner et al 1998b).

The power going into driving a steady wind may be written as

$$L_{\rm wind} = \dot{M}\left(v_{\rm esc}{}^2/2 + v_\infty{}^2/2 + \frac{3}{2}c_T{}^2 + X\right), \qquad (2)$$

where X may include turbulent, magnetic, or wave energy per unit mass. For cool star winds, unlike hot stars, the dominant term is usually the first one that gives the gravitational potential energy that must be supplied to lift the material to infinity, and $L_{\rm wind} < \dot{M} v_{\rm esc}{}^2$. In the Sun, the mechanical energy flux into the chromosphere exceeds that involved in driving the wind by about an order of magnitude, and the power going into driving the wind directly is about 10^{-6} of $L_{\rm Sun}$ (Withbroe 1988, Withbroe & Noyes 1977).

Numerous studies have demonstrated that depositing momentum or energy in the atmosphere below the critical point will tend to increase the mass loss rate, whereas depositing it above the critical point tends to increase the flow velocity more than the mass loss rate. It is difficult to reproduce massive, slow outflows from red giants with stationary wind flow models; the dissipation length or other parameters have to be fine-tuned to deposit enough energy and momentum below the critical point to drive a massive flow, and not too much above it to keep the velocity low (Hartmann & Macgregor 1980, Holzer 1977, Hammer 1982).

Acoustic waves can both heat and impart momentum to the flow. It is common to treat this by including wave pressure terms in the steady wind momentum equation and/or the energy equation. Quite a few varieties of acoustic wave models have appeared in the literature in recent years (Ulmschneider et al 1978, Hammer 1982, Cuntz 1989, Cuntz et al 1998, Sutmann & Ulmschneider 1995, Rammacher & Ulmschneider 1992, Pijpers & Habing 1989). Most such models have a problem with the pattern of wave energy dissipation in the atmosphere. If the dissipation is computed from physically based theory, the result typically suggest that radiative losses dominate (because the dissipation occurs deep in the atmosphere where the density is high). If the dissipation is tuned to produce a reasonable wind model, then there is usually a very narrow range of parameters that can be made to fit.

Alfvén-wave–driven wind theories have been quite successful and are the leading candidate to explain the solar wind as well as the winds of warm giants. Alfvén waves dissipate much less readily, so they can deposit energy and momentum farther out and not lose so much to radiation. If there is a problem with Alfvén waves, it is that they may dissipate too little; at least in the linear regime, they do not provide much heating. Interesting variations on this theme may be found in Moore et al (1992) and Cranmer et al (1999). Alfvén waves may play a role in driving red giant winds, but they are not necessary and they require additional ad hoc assumptions about the nature and source of the magnetic fields involved.

1.2 Stationary Winds with Dust

Dust grains are very efficient at absorbing and scattering starlight; thus, they pick up momentum from the radiation field under conditions where the gas is effectively transparent. Collisions between dust grains and constituents of the gas transfer the momentum to the gas, thus also driving it from the star. This process may drive mass loss (under extreme conditions that rarely, if ever, occur in real stars) or it may enhance and accelerate the wind (a condition that is quite common). Important early contributions to the study of grains in winds include Gilman (1969, 1972), Salpeter (1974a,b), and Draine (1979).

Most observational studies of dusty, cool star winds have been carried out using stationary flow models. There is a minimum mass loss rate such that dust can form in the outflow, and another minimum mass loss rate that allows enough dust to form deep enough in the atmosphere for the outflow to be driven by the dust. In order for dust grains to form in an atmosphere or a stellar wind, nucleation must occur, and the grains must survive and grow. For them to drive a stellar wind, they must intercept a sufficient fraction of the starlight to accelerate outward, and they must be momentum-coupled to the gas through grain-gas collisions. These conditions have been explored by Gail & Sedlmayr (1987a,b), Netzer & Elitzur (1993), Berruyer (1991), and Hashimoto et al (1990).

In the environments where dust forms, CO is preferred over other molecules involving C or O. Thus, if there is more O than C, essentially all the C will be in CO and the excess O will be available to make oxides such as SiO in the first

steps toward forming silicate grains. For detailed discussion of grain formation—equilibrium and non-equilibrium cases—see Gilman (1969), Salpeter (1974a,b; 1977), Draine & Salpeter (1979), Donn (1978), Nuth & Donn (1981), Draine (1979, 1981), Donn & Nuth (1985), and Stephens (1991). The rate of nucleation has a steep temperature dependence near the saturation temperature at any given density. The saturation temperature for SiO lies in the the range 1100–1500 K for the range of densities expected in the driving zone for massive winds. Silicate grains have lower albedos farther into the IR, so they tend to equilibrate with the radiation field at temperatures below the blackbody temperature. Carbon grains, in contrast, tend to equilibrate above T_{BB}.

S-type stars have C $\approx$ O; in these stars, little C or O is left over for grain-forming molecules. This is consistent with observations. There is a higher percentage of S stars among the Miras with periods around 400 days than among Miras with shorter or longer periods (Motteran 1971). This could be because oxygen-rich stars with periods around 400 days tend to be obscured, while the S type stars have less dusty, more transparent, winds. S stars can show very large mass loss rates (Jorissen & Knapp 1998), but even then they tend to have slower and less dusty winds (Sahai & Liechti 1995).

Several conditions must be met if the grains, once formed, are to survive and grow: (*a*) The radiative equilibrium temperature (T_{RE}) of the grains must remain low enough; (*b*) the gas kinetic temperature cannot get too high for too long; and (*c*) the relative motion of the grains through the gas must not be too fast, or the grains will be abraded by gas-grain collisions. The first condition is easy to achieve, even in variable stars. The second is of interest in pulsating stars, where grains must survive the passage of shocks that raise the temperature of the gas to several thousand kelvins or more. (For a discussion of grain survival in interstellar shocks, see Tielens et al 1994, Tielens 1998, or Draine & McKee 1993.) The third condition sets the maximum size of the grains (Salpeter 1977, Draine & Salpeter 1979, Krueger & Sedlmayr 1997).

In a stationary flow, dust forms where $T_{RE} < T_{saturation}$. For silicates, $T_{sat} \sim 1450$ K if the density is a typical photospheric value of about 10^{-10} gm cm^{-3}, or $\sim$1300 K if the density is below 2×10^{-12}, a more reasonable value for the dust formation region. To get $T < 1300$ K from a star with $T_{eff} > 2600$ K requires a dilution factor $W < 1/16$ or $r/R^* > 2$. Even for a star near the tip of the AGB, the density of a static atmosphere will have decreased to less than the interstellar density well below $r \sim 2R^*$. To drive a dusty wind, then, the stars must be cooler than supposed above, the temperature must be lower than T_{RE} near the star, or the true scale height must be much greater than the static value. The last two conditions are generally satisfied in such a wind once it is established, but this argument shows that it is difficult or impossible to start driving a dusty wind in a static atmosphere.

In order for dust grains to drive or accelerate a stellar wind, they must acquire momentum from the starlight and must share this momentum with the gas. Once the grains are formed, their optical properties determine how effective they will be in driving or accelerating the wind. Tabulations and discussions of the optical

properties of grains may be found in Gilman (1974), Draine & Lee (1984), and Draine & Lee (1987). The dust opacity depends sensitively on the size (and structure) of the grains; for spherical grains with radius a, $\kappa_{dust} = (3Q_{pr}/4a\rho_{gr})\ X_{dust}$ where $Q_{pr} \sim 1$, $\rho_{gr} \sim 1$–3 gm/cm^3, and $X_{dust} \leq 2 \times 10^{-3}\ (Z/Z_{Sun})$ is the mass fraction of condensable material. Most calculations of grain dynamics in stellar wind conditions lead to the conclusion that the maximum size that is achieved is around 0.1 micron, and this agrees with observational estimates (Spitzer 1968, Wolff et al 1998). Thus we can't expect to get a strongly dust-driven wind in an oxygen-rich star unless $L/M > 10^4\ L_{Sun}/M_{Sun}$. This number is consistent with what has been found in detailed numerical models relevant to this case (for example, Gilman 1973; Goldreich & Scoville 1976; Kwok 1975; Tielens 1983; Gail & Sedlmayr 1987a,b; Berruyer 1991; Netzer & Elitzur 1993; Mastrodemos et al 1996). An online database for optical properties of grains is kept at http://www.astro.uni-jena.de.

The preceding condition on L/M is a strong indication that dust is unlikely to be the direct cause of stationary winds from normal stars. The coolest and most luminous stars that show signs of dusty winds are the Miras and OH-IR stars at the tip of the AGB. The theoretical limit to the AGB (where the core mass reaches the Chandrasekhar limit) is at about 50,000 L_{Sun}, and most stars only reach $L = 3000\ L_{Sun}$ ($P = 200$ days for the Miras at the tip of the AGB) to $L = 6300\ L_{Sun}$ ($P = 400$ days); see Section 3 and Figure 4.

Further complications attend the theoretical study of grains in stellar winds. In stars where dust grains form and influence the flow, the chemistry of the nucleation process is typically not that of thermodynamic equilibrium or a steady state. For example, hydrogen, generally expected to be molecular at temperatures <1500 K, may be dissociated by periodic shocks and may not have enough time to recover between the shocks (Bowen 1988). This complicates the calculations considerably. For recent work on the nucleation and growth of grains in an environment with $C/O > 1$, see Cadwell et al (1994) or Patzer et al (1998).

From the preceding discussion it appears most likely that steady winds driven by dust alone are rare or nonexistent. Perhaps that should not surprise us. Dust is observed to form primarily—perhaps only—in stars with well-established departures from a steady state, including the pulsating AGB stars, RV Tauri variables, supernovae, and novae. Even for the R CrB stars, whose erratic minima have long been understood to be associated with the formation and ejection of dust clouds, an underlying pulsation has been found to correlate in phase with the onset of a dust episode (Pugach 1977, Holm & Doherty 1988, Asplund 1995).

1.3 Winds from Pulsating Stars

Pulsation can drive or enhance a stellar wind in several ways. First, it provides a natural source of mechanical energy for heating the atmosphere. Second, the atmosphere is "levitated"—given a larger dynamical density scale height $(\mathrm{d} \ln \rho/\mathrm{dr})^{-1}$—by the pulsation, so it partially overcomes the gravitational potential and makes higher density material available for an outflow. Third, departures

from radiative equilibrium lead to refrigerated regions where molecules and dust can form much closer to the star than they would in a static atmosphere or stationary outflow.

Pulsation gives rise to standing or traveling waves, depending on the period of the oscillation. Longer period oscillations, trapped in a resonant cavity, are more likely to result in large-amplitude standing waves. As stars travel up the AGB, fundamental mode pulsation is increasingly favored by these and other considerations. (Wood 1974, 1990; Ostlie & Cox 1986; Bowen 1990).

Waves traveling through decreasing gas density steepen to form shocks. Even for trapped modes, nonlinear excursions of the atmosphere give rise to shocks that propagate out into the atmosphere. If the density gradient were to remain that of the static atmosphere, the shock amplitudes would increase (to conserve energy) until the shocks no longer satisfied the periodicity condition for ballistic motion (Hill & Willson 1979, Willson & Hill 1979):

$$v_{esc}\frac{P}{2r} = 38.3Q = \left[\frac{\beta}{1-\beta^2}\right] + (1-\beta^2)^{-\frac{3}{2}}\arcsin(\beta) \qquad (3)$$

Here, $\beta = v_{out}/v_{esc} = (1/2)\,\Delta v_{ballistic}/v_{esc}$, since in the ballistic case $v_{out} = -v_{infall} = \Delta v_{max}/2$, and $Q = P\sqrt{\overline{\rho}/\overline{\rho}_{Sun}}$ is the "pulsation constant" expressed in days. Observed velocity curves of pulsating stars with shock discontinuities or line doubling indicating the presence of shocks, and with apparently constant acceleration between shocks, have often (but incorrectly) been interpreted as yielding a direct measure of the surface gravity, g. The maximum ballistic shock amplitude is approximately equal to g P for short periods, but for $Q \sim 0.03$–0.1 day, which is characteristic of most radially pulsating stars, $\Delta v_{max}/g\,P < 0.8$ to 0.4. The amplitude is further reduced by including the effects of pressure gradients acting between shocks. If, instead of assuming ballistic motion, we integrate the equation of motion over a cycle and again invoke periodicity, we find that the expected pattern is asymmetric, with $v_{infall} > v_{out}$, as given by Willson & Bowen (1984a):

$$\begin{aligned} {v_{infall}}^2/{v_{esc}}^2 &= {v_{out}}^2/{v_{esc}}^2 + \left(2{c_T}^2/{v_{esc}}^2\right)\ln(\rho_o/\rho_f) \\ &= \left({v_{out}}^2/{v_{esc}}^2\right) + (H_{static}/R)\ln(\rho_o/\rho_f) \end{aligned} \qquad (4)$$

For strong adiabatic shocks, $(\rho_o/\rho_f) = 4$; for isothermal shocks it can be much larger. This term typically introduces a correction on the order of 5–10% for periodic motion in the Miras; the magnitude of this effect is less for stars of higher gravity. An indication of the importance of the pressure gradient between shocks is the inequality between the blue- and red-shifted components, which is striking for Miras but not evident for higher gravity stars (Willson et al 1982, Hinkle 1995).

Material given an impulse greater than $v_{esc}\beta$ at time t_s does not have time to return to the same position before the next shock passes at t_s+P. The result is a net outward displacement of material until the density gradient has become sufficiently shallow that the shocks can satisfy Equation 3. Thus the atmosphere is

extended—levitated—by a combination of the kinematic fact that the average position of a mass element is significantly outside its minimum distance, and the need for the shallower density gradient to satisfy the energy and periodicity conditions.

Once the shock amplitude has reached the periodic limit, the material may be unable to radiate enough energy between shocks to return to the radiative equilibrium temperature. As a result, a region with persistent $T > T_{RE}$, a "calorisphere," may form, allowing all the energy dissipated in shocks to be radiated away. Farther out, the density becomes low enough that the only way the atmosphere can maintain a steady state (averaged over the pulsation cycle) is for the extra entropy introduced by each shock to be advected outward in a slow flow at roughly constant velocity (Struck et al 2000, in preparation). In Bowen's numerical models (1988; 2000 in prep) this behavior is seen in cases where dust does not form (see Figure 1, lower panel) where the outflow remains steady out to tens of stellar radii, with $v < c_T \ll v_{esc}$. Thus, circumstellar lines with low flow velocities may arise from a subsonic outflow that need not have $v > v_{esc}$ as long as there are waves propagating through it. Note that even with such slow flow there is no sign in any theoretical models of stationary layers or shells such as those supposed to exist by several groups interpreting observational data (see, for example, Hinkle et al 1982, Reid & Meuton 1997).

The temperature structure in the atmosphere is determined by a combination of the expansion (adiabatic or hydrodynamic cooling) and interaction with the radiation field. To treat the coupling of the gas with the radiation field is not a simple matter, even for local thermodynamic equilibrium (LTE). Below about 8000–10,000 K the cooling is dominated by a variety of neutral "metals" and molecules. Hydrogen becomes important around 10,000 K, and in the typical situation the Lyman lines and possibly some of the Balmer lines will be optically thick over a short distance in the atmosphere. The problem is most difficult between the simpler extremes of LTE in deep stellar atmospheres and extreme non-LTE in the interstellar medium. However, some simplification is possible. For a two-level atom with critical density ρ_x the line source function is reduced below its LTE value by $S/S_{LTE} = 1/(1+\rho_x/\rho)$. For each transition important in the radiative transfer there is a critical density where this occurs; the gas as a whole behaves to first order as though it had a critical density (ρ_x) at a value characteristic of the most important radiative transitions. Thus, at low densities, the cooling is proportional to the collision rate in the gas. This provides a convenient parametrization of the more realistic case, where many transitions are involved, leaving only the problem of selecting an appropriate value for ρx. (For discussion of this point, see Willson & Bowen 1998; see also Woitke et al 1996, but note that their analysis implicitly assumes very narrow intrinsic line profiles and continuum opacity $\ll$ line opacity, both conditions that probably do not apply in red giant stars and that overestimate the importance of photon trapping.)

Figure 2 shows the difference in the atmospheric temperature structure for two cases that are identical except for the value chosen for ρ_x. In the bottom panel,

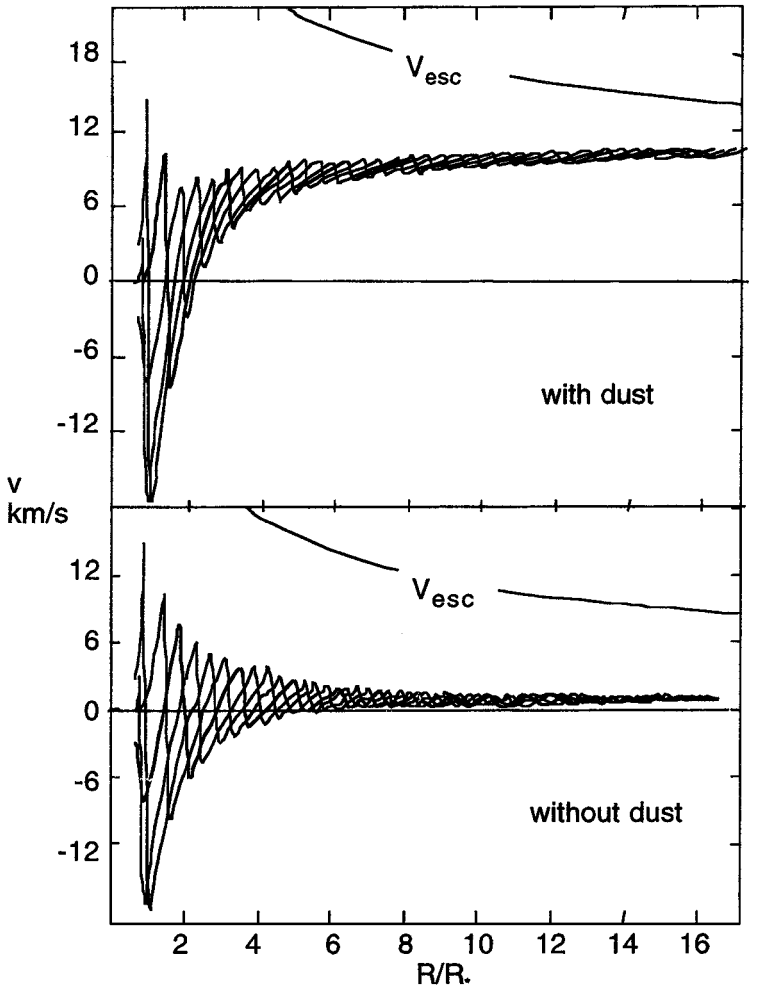

Figure 1 Velocity as a function of radius for two models differing only in that for the top panel, dust formation is allowed, whereas for the bottom panel, dust formation has been artificially suppressed. The slow, constant velocity outflow in the bottom panel is also commonly seen in models that are allowed to make dust but do not reach the right conditions—low-metallicity, low-mass, and/or low-luminosity models. (Figure courtesy of GH Bowen.)

small ρ_x, most of the atmosphere has $S \sim S_{LTE}$ and is able to return to radiative equilibrium quickly. If ρ_x is high (top panel), the partial decoupling of the gas temperature from the radiation field provides for regions with $T < T_{RE}$ as well as regions with $T > T_{RE}$. This is important for dust and molecule formation close to the star, and is discussed in more detail below.

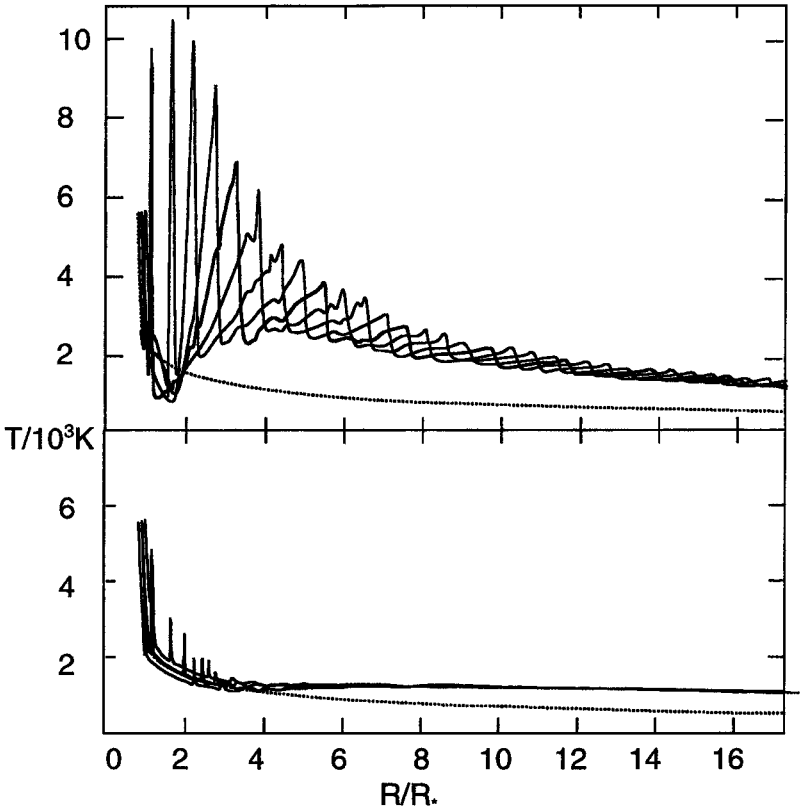

Figure 2 Temperature versus radius from two models that are identical, except that in the top panel the critical density $\rho_x = 10^{-10}$ gm cm^{-3}, while in the bottom panel $\rho_x = 10^{-18}$ gm cm^{-3}. Lower critical density results in a more extended region where $T \sim T_{RE}$ between shocks. (Figure courtesy of GH Bowen.)

Given the difficulty of carrying out non-LTE radiative transfer in the context of an extended, dynamical atmosphere it is tempting to try LTE transfer using the temperature and density structure derived from a dynamic model to compute predicted spectra. However, this approach overlooks the importance of matching the assumptions in the radiative transfer code to those of the dynamical calculation. If LTE transfer is used on a hydrodynamic model that used non-LTE cooling, then the transfer code assumes that there is a lot of energy stored in excitation that in the dynamic model went into thermal kinetic energy and/or mass motions. Thus, the LTE transfer in this case will produce an overabundance of photons from some parts of the model by violating conservation of energy. For a dramatic example of the results of such a mismatch, see Bessell et al (1989, Figure 25). Similarly, because the conditions that lead to non-LTE level populations are the

same as those that lead to departures from radiative equilbrium in a non-static atmosphere, it is inherently inconsistent to put non-LTE into a hydrodynamic code and then insist on radiative equilibrium.

1.4 Pulsating Stars as Dust Factories

Pulsation and dust formation together characterize the bulk of the Miras and OH-IR stars that are clearly losing mass at a rapid rate. Theoretical evidence of this is as follows: Very extreme conditions would be required to allow dust to drive the wind alone, whereas the formation of dust in a pulsating star can greatly enhance the mass loss rate over what it would be if dust did not form. Also, departures from radiative equilibrium in the atmospheres of pulsating stars can enhance the rate of dust formation. Observational evidence is as follows: All the stars in which dusty winds are evident are also pulsating. The properties of the wind correlate strongly with the pulsation characteristics, even for stars with the same period of pulsation; as Bowers & Kerr (1977) pointed out, the heaviest mass loss comes from stars with the most asymmetric light curves, all else being approximately equal. Narrow 10 μm features occur preferentially at a particular phase, indicating variation in the properties of the dust grains with phase (Monnier et al 1998).

In Figure 3, the location of the "dust factory" region is sketched for one of Bowen's (2000 in prep) model Miras. In the darkly shaded region the pressure exceeds the saturation pressure by four or more orders of magnitude, suggesting that nucleation should be rapid. The dust nucleated in one cycle acquires a small outward velocity relative to the gas; only when the dust has reached a size approaching a tenth of a micron does this relative velocity become appreciable. The coupling of the dust and the gas creates the net outflow shown in Figure 1, where it is contrasted with the velocity structure in an otherwise identical model where dust formation has been artificially suppressed. Clearly, the outflow velocity, and hence the momentum of the wind, is determined by the action of the radiation field on the dust. Thus it should be no surprise that most Miras and OH-IR stars satisfy $\dot{M}\, v_\infty < L/c$, and a few even exceed this condition (possible for multiple scattering in a nearly optically thick wind); see, for example, Knapp (1986). Note also that nowhere in the atmosphere is there any kind of "stationary layer"; the illusion of such a layer is presumably produced by the fact that at all phases there is material with $dr/dt \sim 0$, and that this material is in about the same phase of the expansion-cooling cycle at all phases.

The ideal model for the wind from a pulsating star would be one in which (*a*) the driving zone and the atmosphere are treated together in a consistent way; (*b*) the temperature structure is computed using full non-LTE transfer in the radiation hydrodynamics; (*c*) the shocks are fully resolved in space and time; (*d*) the non-equilibrium molecular chemistry, dust nucleation, dust-gas interactions, and resulting energy exchange are followed in full non-equilibrium; (*e*) the model extends to at least tens and preferably hundreds of stellar radii. Such a model is not available now nor likely to be forthcoming any time soon. The

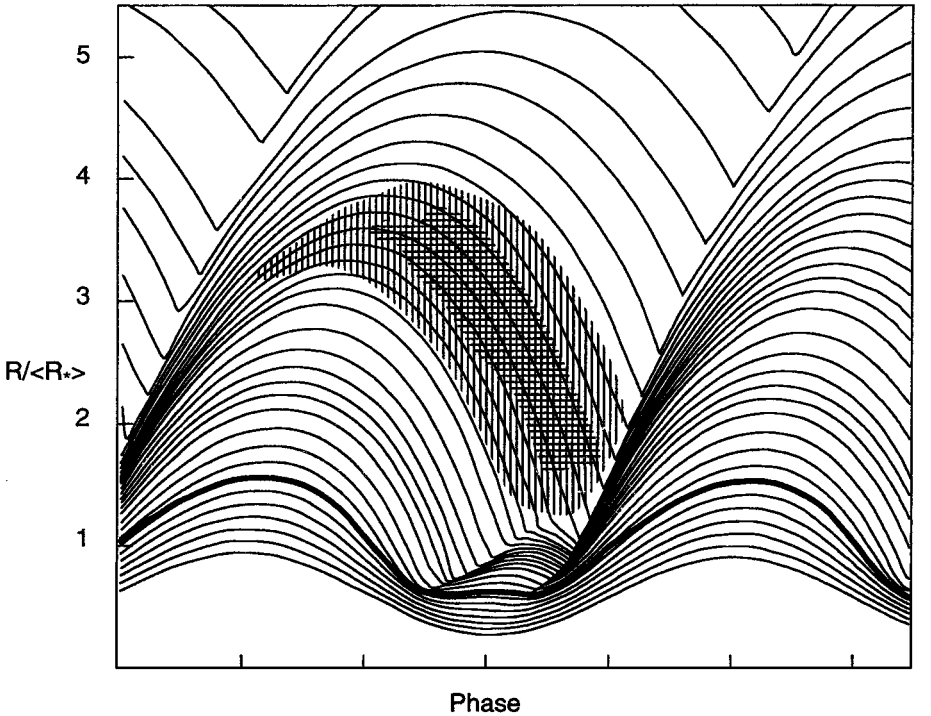

Figure 3 Radius as a function of time for a representative selection of atmospheric zones, with the "dust factory" region of a model indicated by the shaded areas. In the "dust factory," the pressure exceeds (by orders of magnitude in the darker region) the saturation pressure, and nucleation of grains is expected to be rapid. (Figure courtesy of GH Bowen.)

models that are available roughly fall into two categories: those that include some of the above processes in exhaustive detail and drastically approximate others, and those that use just-adequate approximations for as many of these processes as are needed to produce a reliable series of models.

Bowen's (1988; 2000, in preparation) models for the oxygen-rich Miras typify the second approach. His energy computation includes an Eddington-approximation grey spherical atmosphere calculation with constant opacity to determine the radiative equilibrium temperature. Relaxation toward that equilibrium temperature is determined by rates that come from a detailed computation for hydrogen cooling at high temperatures, and an approximate cooling coefficient derived from other sources that is used at lower temperatures. His dust formation is parametrized, although the region where dust forms is found after the calculation to correspond closely with the region where the SiO is supersaturated. The exchange of energy and momentum between the gas and dust is considered in some detail. The models extend to tens of stellar radii and a few have been computed to hundreds of stellar radii. All approximations used have been tested for their

effects on the mass loss rates and have been found to have modest effects over a range of reasonable parameter values. Thus, Bowen's mass loss rates are probably reliable to $\sim\pm0.5$ dex for a given set of stellar parameters. As is demonstrated in Section 3, this is sufficient accuracy for deriving the pattern of late AGB mass loss and determining the properties of stars when they reach the stage of high mass loss rates.

Early studies of pulsating atmospheres in Miras by Hill & Willson (1979; also Willson & Hill 1979) and by Wood (1979; also Fox & Wood 1985) demonstrated that fast relaxation ("isothermal") shocks gave rise to little or no net outflow, whereas entirely adiabatic shocks caused the atmosphere to simply blow up. Hill & Willson recognized that slow relaxation (and thus an approach to adiabatic shock conditions with decreasing density) would give the right order of magnitude of mass loss rates. Wood was the first to explore the coexistence of shocks and dust grain formation in a Mira atmosphere; he also carried out studies of the internal pulsation and tried to establish the pulsation mode from observational constraints on the radii and masses of Miras. Hill & Willson also pointed out the difficulty of reconciling observed shock amplitudes (from infrared CO line studies; Hinkle 1978, Hinkle & Barnes 1979a,b) with overtone pulsation.

Sedlmayr and his collaborators have concentrated on the chemical reactions that lead to grain nucleation and growth, initially in the context of steady outflows and more recently for pulsating stars (for example, Winters et al 1997). They are systematically investigating a range of relevant phenomena, and their models are converging toward greater similarity with Bowen's results (making due allowance for the differences between carbon-rich and oxygen-rich chemistry) as they incorporate more of the essential physics. Most of their early work dealt with the chemistry and dynamics of atmospheres with C/O $>$ 1 (often substantially greater than 1) because it is not possible to drive a stellar wind by the action of radiation pressure on grains unless C/O is large and the star is very luminous and very cool. The importance of carefully treating the opacity in the deeper (LTE) layers of the atmosphere is addressed in Höfner et al (1998a,b). Predicted spectral variations are compared with observations in Hron et al (1998, Loidl et al 1999).

A very strong dependence of the mass loss rate on stellar parameters emerges from theoretical studies (Bowen & Willson 1991, Höfner & Dorfi 1997). If a set of evolutionary tracks is expressed by setting the radius (or $T_{\rm eff}$) equal to a function of L, M, and Z, then the parameter dependence can be reduced to mass loss rate as a function of L, M, and Z for stars evolving up the AGB. In the top panels of Figure 4, the dependence of $\dot{M}$ on L is displayed for (*a*) solar composition and five masses and (*b*) one solar mass and five metallicities, from Bowen models using evolutionary tracks from Iben (1984) with mixing length parameter $\alpha = 0.9$.[1] At a given L

[1]Note that the Iben mixing length formulation is slightly different from the Cox & Giuli (1968) formulation often used, so an Iben mixing length of 0.9 produces models with characteristics similar to a Cox & Giuli formulation with $\alpha = 1.5$ or more (see, for example, Becker & Iben 1979).

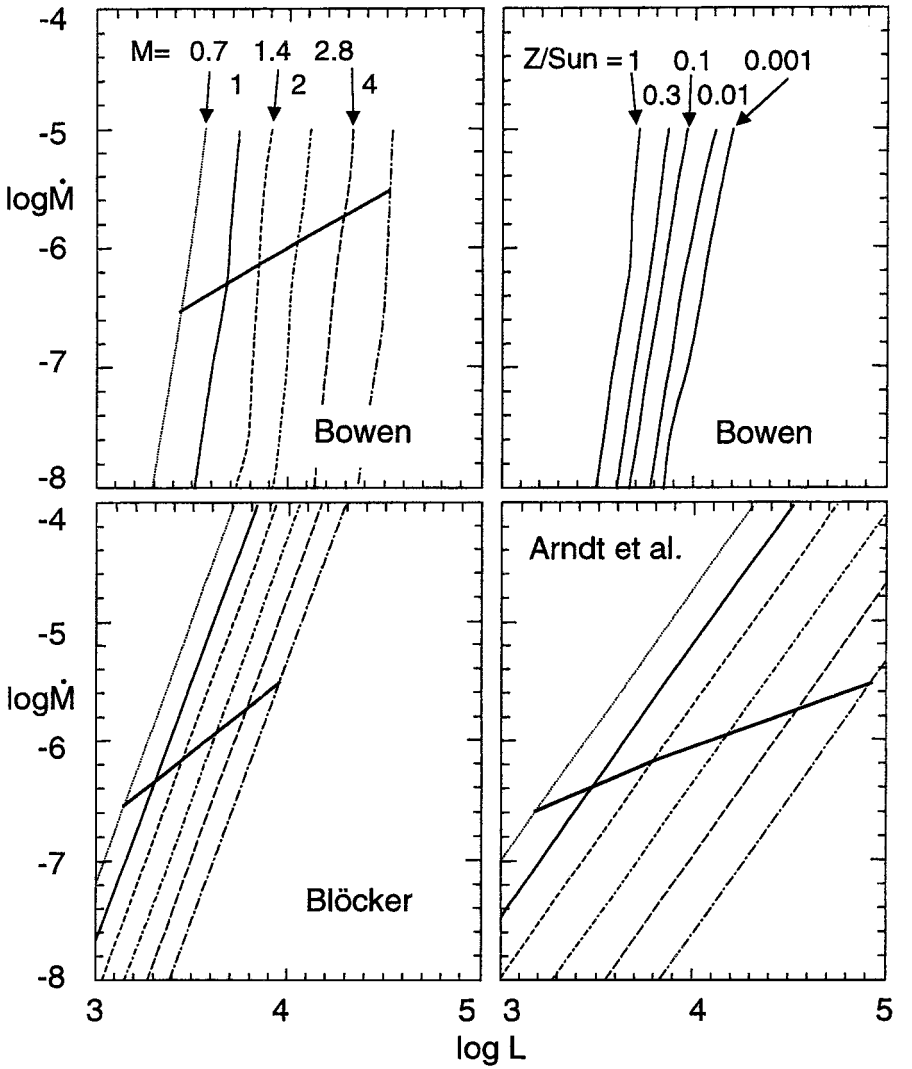

Figure 4 Mass loss rate vs. luminosity using four theoretical mass-loss relations with a single set of evolutionary tracks (Equation 7). *Top panels*: Models by Bowen (1995, unpublished; 2000, in preparation) for six masses with solar composition (*left*) and 1 M_{Sun} with five metallicities (*right*). *Lower panels*: Mass loss relations by Blöcker (1995) and Arndt et al (1997) for the same six masses. In each panel the locus of critical mass loss rate, $-\mathrm{d} \log \mathrm{M}/\mathrm{dt} = \mathrm{d} \log \mathrm{L}/\mathrm{dt}$, is indicated.

and M, the lower Z models have much lower mass loss rates, but even very low Z stars can achieve high mass loss rates when they become sufficiently bright. Lower metallicity stars have lower mass loss rates mainly because they have smaller radii at a given M and L; the effect of dust is secondary (Bowen 2000, in preparation; Willson et al 1996). On each of these plots is a line indicating the critical mass loss rate ($-\mathrm{dM/dt} = \mathrm{M/L\ dL/dt}$) at which mass loss begins to dominate the evolution (see Section 3). Observational selection will favor observations of stars with long mass loss timescales and high mass loss rates—i.e. stars near the critical mass loss rate. The lower panels of Figure 4 show similar plots using the mass loss formula of Arndt et al (1997) for carbon-rich models and using the formula derived by Blöcker (1995) from the 1988 Bowen models. (The models Blöcker used were not yet constrained according to the energy condition on the "piston" amplitude that has since proved useful, therefore the results are not the same as in the current Bowen grid used in the top panels of Figure 4.) At the end of Section 2 you'll find a similar series of plots for a variety of "empirical relations" that are in common use.

2. OBSERVATIONS OF MASS-LOSING GIANT STARS

In his review entitled "Mass loss from stars" for *ARAA* in 1963, Weymann wrote, "One gets the impression that in many aspects of the subject the number of pages expended in reviewing the subject ... probably exceeds the number of pages of material being reviewed." That is definitely not the situation now. Fortunately, there are also a number of recent reviews covering aspects of the subject very well. Knapp (1991) clearly described a variety of methods for detecting and measuring mass loss from evolved stars, and Van Der Veen & Rugers (1989) compared mass loss rates derived by molecular line and infrared techniques. Olofsson (1996a,b; 1997) reviewed the structure of the circumstellar envelope and its molecular chemistry. Dupree (1986) examined the techniques based on spectral lines in the UV and optical. Infrared methods have been reviewed by Bedijn (1987), high spatial resolution observations by Dyck (1987), and mass loss in general by Lamers & Cassinelli (1996, 1999). In this section, I stress a few points of particular relevance to the derivation of mass loss laws, the evaluation of theoretical mechanisms, and the determination of the properties of mass-losing stars.

2.1 Methods for Determining the Mass Loss Rate

The number of papers concerning mass loss from cool stars rose precipitously with the appearance of data from the IRAS satellite. The IRAS color-color plot was found to be a very useful tool for diagnosing and classifying at least the dusty winds from very evolved stars (Van Der Veen & Habing 1988). Most of the evolved sources fall along a band of increasing $\log(F_{12\mu m}/F_{25\mu m})$ that represents increasing rates of mass loss for M and C stars, with the larger amplitude pulsators also tending to cluster in the higher mass loss classes. The population of the part of the diagram with 60 μm "excess" is most readily interpreted as the result of the

cessation or substantial reduction in the rate of mass loss, so that the expanding shell cools. It appears most likely that these shells represent peaks in the mass loss rate associated with shell flashes, possibly further compressed by variations in the wind speed (Chan & Kwok 1988; Olofsson et al 1990, 1998).

An unambiguous indicator of circumstellar matter, hence mass loss, is the appearance of the 10–15 μm "bump" (or dip, if in absorption) characteristic of the opacity of silicate grains (10–12 μm) and carbon grains (13–15 μm). Infrared measures of the mass loss rate generally depend on fitting models to the observations. Typically, models assume constant outflow velocity, parametrized by dust/gas ratio, optical depth, and inner dust radius or maximum dust temperature. The fits are most sensitive to the inner dust radius and temperature. Published fits have not always taken into account that the dust temperature, if silicate dust is involved, will be below the blackbody radiative equilibrium temperature (see Section 1). There is a close correlation between the appearance of the 10 μm, i.e. the optical depth of the envelope, and the K-L color; this correlation may be translated into a very convenient relation between K-L and mass loss rate (Lepine et al 1995, Jones et al 1990).

The basis for deriving mass loss rates from radio molecular lines is described and illustrated in a series of papers by Knapp (1986) and Olofsson (1996a,b; 1997), and also by Nyman et al (1992), Wannier & Sahai (1986), Wannier et al (1990), Sahai & Wannier (1992), Little-Marenin et al (1994), and Sopka et al (1989). Mass loss rates derived this way do not always agree with those derived from IR or near-IR photometry, but this may well be for good physical reasons rather than because there are flaws in any one method. For CO-line fitting, the parameter to which the result is most sensitive is the *outer* radius of the CO shell, because it is the volume of the CO shell (along with mass loss rate) that sets the amplitude of the signal. This outer radius, typically 10^{16} to 10^{17} cm, is usually set by the location where photo dissociation by interstellar UV photons becomes important—although in rare cases it could instead be determined by the time of the onset of a mass loss episode. If the flow is clumpy, the CO mass loss rate derived from the standard equations will underestimate the mass loss rate, possibly substantially (Olofsson et al 1992). Also of importance is that these lines give indications about the mass loss rate some time before the present—typically 100 to 1000 years BP—whereas mass loss rates are known to vary on timescales from decades (for reasons not well understood) to thousands of years (over the shell-flash cycle).

Many of the stars that are losing mass most rapidly are also maser sources. Maser emission has been recently reviewed by Elitzur (1992). Briefly, SiO maser lines appear to originate from about the same location in the atmosphere where grains form, around 1–3 stellar radii, where they can be pumped by collisions; this is confirmed by the correlation of the SiO maser variability with the phase of pulsation (Herpin et al 1998, Gray et al 1999, Humphreys et al 1997a,b). For Miras and semi-regular long period variables, interferometric studies have demonstrated that the H_2O maser emission originates from a region $\sim$5–10 $\times$ 10^{14} cm in radius centered around the star, whereas OH masers form much farther out in the wind, typically

at distances of $>10^{16}$ cm, where H_2O has been photo-dissociated by interstellar UV photons. The OH maser lines have provided useful data on mass loss rates and, in particular, on outflow velocities at very great distances from the star.

Recently, images of mass-losing stars taken in the scattered light of atomic resonance lines of potassium and sodium have indicated (*a*) that these atoms are not heavily depleted onto grains in the outflow, and (*b*) that the envelope is also not heavily ionized by stellar UV from a stellar chromosphere (Gustafsson et al 1997, Guilain & Mauron 1996). The light from Miras is sometimes found to be polarized, with heavy dependence of the polarization on the wavelength (Coyne & Magalhaes 1977, 1979; McLean & Coyne 1978; Codina-Landaberry & Magalhaes 1980; Kruszewski et al 1968; Boyle et al 1986). No existing model gives a full explanation for these effects, but the scattering of photospheric photons by electrons or dust in the circumstellar envelope and wind appears most likely to be responsible.

Radio continuum measurement of mass loss rates has been a powerful tool for hot stars and has been applied with mixed success to cooler ones. Post-AGB stages were detected by Spergel et al (1983) and Knapp et al (1995). Several K and M giants were detected in a study by Drake et al (1987, 1991); 1.3 mm continuum emission has also been detected from mass-losing AGB stars by Walmsley et al (1991). Reid & Menten (1997) determined that several long-period variable stars had thermal radio emission with a spectral index $\sim$2, characteristic of an optically thick thermal source. They interpreted this result as evidence for a "radio photosphere" and developed a detailed empirical model; however, the same data may be interpreted with quite a different model based on rising shock fronts in a dynamical atmosphere (Willson 1999).

2.2 Observations of Mass-Losing Stars with High Spatial Resolution

In theoretical models, the inner radius at which dust forms depends on the luminosity of the star, the nature of the dust, and the local gas temperature. While the nature of the dust can be constrained by general arguments, the local temperature depends strongly on the modeling methods used. Thus, observational constraints on the inner dust radius and/or the maximum temperature of the dusty shell are very useful for comparison with modeling results. Bester et al (1991) found that the inner dust radius for o Ceti was around 3 stellar radii, corresponding to a radiative equilibrium temperature around 1200 K; this is in agreement with theoretical expectations (Section 1), although this temperature is higher than has been used in many IR-fitting models (see also Danchi et al 1994, Danchi & Bester 1995).

HST observations of proto-planetary nebulae have revealed two further intriguing facets of late-AGB mass loss, also confirmed by interferometric studies (Lattanzi et al 1997). The mass loss appears to retain predominantly spherical symmetry until the very last moments of AGB outflow, when bipolar symmetry typically emerges (Skinner et al 1997). A simple examination of the ways in which an outflow may become axially symmetric reveals quickly that for a single star,

until the envelope mass is very small, an impossibly large amount of angular momentum will be required to modify the flow (Willson & Bowen 1988). The more surprising fact emerging from these studies is that the outflow before this stage appears to be modulated on a timescale of decades to centuries—too short for the shell flash cycle, and too long for the pulsation cycle (Skinner et al 1997). Many of the pulsating AGB stars show modulations in their periods and/or their amplitudes on a similar timescale (Percy & Colivas 1999); these modulations are not yet well understood. This timescale is about the same as the thermal (Kelvin-Helmholtz) timescale for the envelope or the orbital periods for solar system–like planets.

2.3 Determination of the Properties of Mass-Losing Stars

Properties of mass-losing stars that we would like to know accurately include the luminosity, the radius, and the mass. Most methods for determining L and R require that we first determine the distance to the system. In addition, for studies of the evolution of stellar populations, we need to determine the dependence of the mass loss rates, or the properties of mass losing stars, on the metallicity.

2.3.1 Distances and Luminosities The Miras in the LMC have been extensively studied (Glass et al 1987, Mould & Reid 1987, and Hughes & Wood 1990). The P-L relation for Miras in the LMC is shown in Figure 5, with the individual stars taken from Feast et al (1989); an entirely similar plot results from using data from Hughes & Wood, who observed a larger sample of stars. In this figure, the theoretically expected P-L relation (derived from the analysis in Section 3) is also shown. Feast preferred a single linear fit to the data that has been widely used as the Mira P-L relation. However, the excellent match between theoretical models and the observed P-L relation supports the contention that the "corner" in the relation is real and comes from the much weaker dependence of the effective temperature on stellar mass below about 1 M_{Sun} seen, for example, in the models of Iben (1984, and sources therein).

Obtaining the distances to Miras in our own galaxy is difficult; very few of the highly evolved AGB stars are located close enough for traditional parallax measurements. The Hipparcos list included a few Miras, as well as closely related semi-regular variables, with simultaneous ground-based observations and analyses of the light curves as a bonus. The results that have been derived from data obtained by the Hipparcos satellite have profoundly affected our confidence in the distances to a wide variety of stars. What is less widely appreciated is that the method used by the satellite to establish the positions of stars has some problems when the source becomes extended, and in particular has a very limited range of parallaxes to which it is sensitive when the object being measured is $>$1AU in radius. This, of course, is the case for nearly all the evolved red giants that are losing mass—radii cited in the literature range from 1 AU upward to several AU for stars near the tip of the AGB. Wallerstein & Knapp (1998) found that Hipparcos parallaxes to carbon stars were reliable only when both $\varepsilon(\pi) < 1.75$ mas and $\pi/\varepsilon(\pi) > 3$,

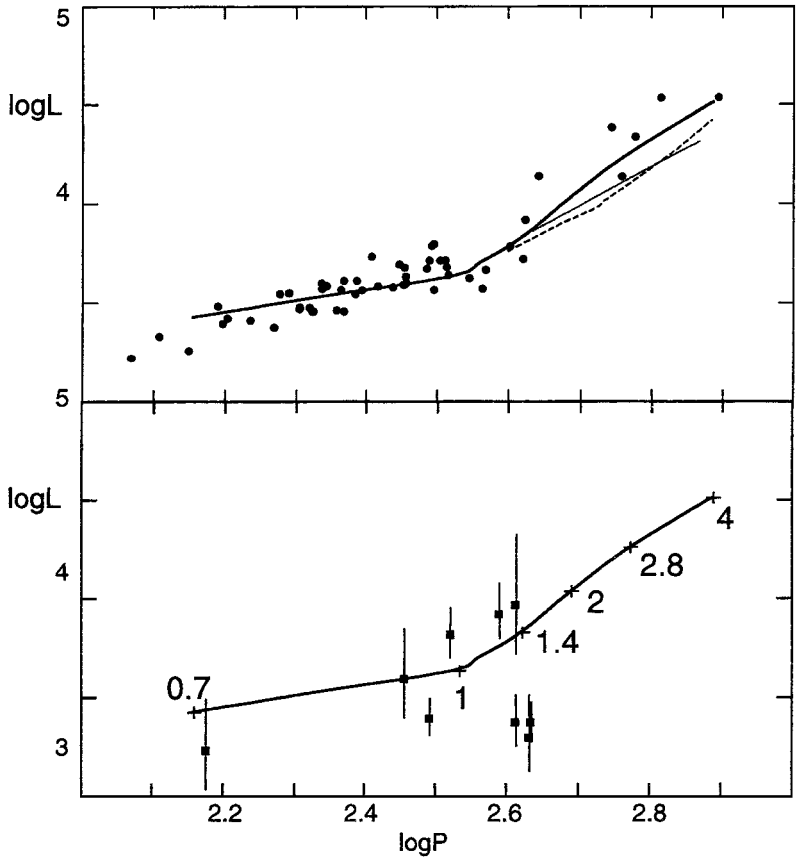

Figure 5 Period-luminosity relations for Mira variables. *Top panel*: Measured luminosities and periods for LMC stars from Feast et al (1989) with the theoretical locus derived in Section 3 superimposed. *Solid line*: Z/Zs $= 1$. *Dashed and dotted lines*: $Z/Z_{\odot} = 0.3, 0.1$. *Lower panel*: The same theoretical locus is shown with galactic Miras, using Hipparcos parallaxes from Van Leeuwen et al (1997), selected as described in the text.

where π is the parallax and $\varepsilon(\pi)$ is the error in π. Applying the same criterion to the Miras and SR variables observed by Hipparcos and reported by Van Leeuwen et al (1997) leaves a total of seven M Miras, one S Mira, and (after adding two stars from Wallerstein & Knapp's list) three C Miras with presumably reliable Hipparcos distances. These are all shown in the lower panel of Figure 5, where the theoretical P-L line from the top panel is also reproduced. The scatter is large, as are the error bars. The only star on the line is one that is most likely to deviate: R Aql, a star experiencing rapid change in its period (and therefore its radius as well) presumably in response to a shell flash (Wood & Zarro 1981). The scatter is unlikely to result from differences in metallicity, since the P-L relations for

$Z/Z_{Sun} = 0.1$–1 nearly coincide (upper panel of Figure 5). The P-L relation from the LMC is probably still a better guide to distances for Milky Way Miras than are the Hipparcos parallaxes. The width of the relation in log L is about 0.2dex; this is not likely to be reduced much by further observations, since it is already about the width expected from the lifetime of the Miras (Section 3).

Another technique for determining the distance to a star with an OH maser is to look for time delays between maser emission coming directly to us and that bouncing off the back of the shell first. If the angular diameter is also known, this yields a direct measure of the distances (Van Langevelde 1990). The OH-IR stars have been suggested to comprise an extension of the Mira P-L relation to higher luminosities. Some of the OH-IR stars with higher-mass progenitors do appear to extend P-L relation. However, it has been clearly demonstrated for infrared LMC sources, as was expected from theoretical arguments, that most of the heavily obscured sources are at the same L but longer P, thus corresponding to evolution to lower mass at roughly constant or declining L during the heavy mass loss stage (Wood 1998). Many of the papers in the literature concerning properties of OH-IR stars have assumed that the luminosity of an OH-IR source is approximately 10^4 L_{Sun}; these analyses should be redone with better luminosities as those become available.

2.3.2 Angular and Linear Diameters In the last decade there has been a steep increase in the number of angular diameters reported in the literature based on a range of mainly interferometric techniques, with multi-element interferometers gradually dominating over speckle and occultation methods. (See, for example, Ridgway et al 1979; Bonneau et al 1982; Haniff et al 1995; Lattanzi et al 1997; Van Belle et al 1996, 1997; Danchi et al 1995; Karovska et al 1991.) On rare occasions, these methods yield direct images or brightness distributions sampled along two perpendicular directions; more often, it is necessary to work with a one-dimensional (sampled or integrated) brightness distribution and to fit a simple model of the expected brightness distribution to the observations. Early work often used uniform disk models and/or models with a standard limb-darkening function applied. More recently, some teams have been using detailed radiative transfer computations linked to dynamical model calculations from Scholz & Takeda (1987), hoping to achieve increased accuracy; however, the fact that those models do not include the layers most likely responsible for circumstellar scattering (the ionized calorisphere and the dusty wind) is cause for concern. There is some evidence that a Gaussian profile may fit better than any of the standard models (Van Belle et al 1996), suggesting that circumstellar scattering may be an important factor. As was pointed out by Tsuji (1978), a modest amount of circumstellar scattering can have no discernable effect on the spectral energy distribution or line spectrum, while greatly affecting the determination of the angular diameter by any interferometric method. Perrin et al (1999) concluded from a detailed analysis of observations of R Leo that nearly all means of improving the fit to interferometric

observations would reduce the angular diameters derived; they favored scattering over most other interpretations for their data. A great advantage of publishing uniform disk angular diameters is that it makes it much easier to reinterpret the data in the light of new models.

In theoretical models, the density declines exponentially in the vicinity of the photosphere, just as it would in a static model. The variation in the photospheric radius over the pulsation cycle is typically no more than $\pm 15\%$ (see Figure 2). The photospheric exponential decline in density goes over into a roughly $1/r^2$ decline a few tenths of a stellar radius above the photosphere; the density at which this occurs is determined by the mass loss rate. If the photosphere is truly what is being observed, then the observations should show time variability not exceeding $\pm 15\%$ from the mean, and wavelength variation significantly less than this at any given phase. The observed variations are much larger; therefore most of these observations are probing the wind, not measuring the star. The observed strong wavelength dependence of the derived stellar sizes, even for non-variable red giants (Quirrenbach et al 1993) but more extreme for Miras (Bonneau et al 1982), provides additional support for this point of view, as does the tendency for the resolved image to be non-spherical (Lattanzi et al 1997). If scattering is an important process in the atmosphere, as appears to be likely, then interferometric techniques that are not carefully controlled for polarization bias will tend to produce football-shaped images, with the scattered light being picked up where the polarization angle is right. Also, derivation of an 82% change in the radius of o Ceti over just two years (Tuthill et al 1995) should be a clear indication that the true radius is not being observed. Even for a conservative estimate of the amount of mass involved, the power needed to expand the star by that much so quickly would be greater than the stellar luminosity, and such an expansion on a timescale considerably below the Kelvin-Helmholtz time is also not plausible.

Given L and P, one should be able to obtain an estimate for the radius of the star from theoretical evolutionary models. This is also difficult for evolved, highly convective giants. The radii of AGB stars are ill-constrained by evolutionary models, since varying the mixing length or molecular opacities gives rise to models with very different radii at a given luminosity. Using period-mass-radius relations to estimate the radius depends on knowing the mass of the star and the mode of pulsation; as noted previously, uncertainties in the measured angular diameters are large enough to introduce ambiguity in the assignment of the pulsation mode.

2.3.3 Masses Both observational studies (Clayton & Feast 1969) and theoretical models (Hughes & Wood 1990, Bowen & Willson 1991) agree that the sequence from short to long period in Miras is primarily one of increasing stellar progenitor mass, with individual stars spending $\sim 2 \times 10^5$ years evolving across the P-L band. (This is graphically displayed in Figure 8 of Wood et al 1992.) It appears most likely that the P-L relation is a kind of "main sequence" of the Miras, selected not

according to the nuclear burning process or longevity of the stage but rather by the mode of pulsation and the level of mass loss. While most of these studies do not yet take into account the effects of shell flashing on the appearance, Vassiliadis & Wood (1992) have also explored the consequences for observable properties of Miras—P, $\dot{P}$, $\dot{M}$—of the shell flashes, assuming that the mass loss rate follows the period.

The period-luminosity relation may be our most reliable estimate for the present masses of Miras, and it gives values quite close to those of the progenitor stars as derived from population studies. Other direct measurements of the masses of evolved AGB stars are very few. The *o* Ceti visual binary system, for example, should yield a reliable mass estimate in time, but the estimated orbital period is >200 years. If the P-L relation gives correct masses, then the common assumption that the masses of Miras range from <1 to ~ 1.5 M_{Sun} is good for the stars with periods less than 400 days (with those <300 days most likely having masses <1 M_{Sun}), whereas the longer-period Miras probably have higher masses. Many studies of the properties of Miras and OH-IR stars as a class begin with an assumption—such as that all the stars have masses between 1 and 1.5 M_{Sun}—that is contradicted by the mass assignment shown in Figure 5. Other studies have used assumed mass loss laws and thus derived $M_{present}$ as ($M_{progenitor} - \int_{ms}^{now} \dot{M}\, dt$). Unfortunately, in some cases masses derived this way have been used to calibrate mass loss laws with quite different dependence on stellar parameters than what was used in the above integral—a reminder that it is risky to quote numbers without tracing their origin.

Masses for other cool, mass-losing stars, including the heterogeneous semiregular variables and the supergiants, are quite uncertain at present because the classification of those stars is less definitive and their histories less clear. Most of the SRa and some of the SRb variables are probably AGB stars that have not yet reached the Mira mass loss stage. However, a given star evolves through a considerable range of L before it reaches the relatively narrow L, P of the Miras, so P will not correlate with mass for SR variables as neatly as for the Mira stage. See, for example, Kerschbaum & Hron (1996).

2.4 Modes, Periods, and Period Changes as Clues to the Nature and Evolutionary Status of Miras

An independent estimate for the mode of pulsation, and hence the likely range of radii, may be made from an estimate of the mass of the star and observation of the dynamical behavior of the atmosphere. This approach was first developed by Hill & Willson (1979; see also Willson & Hill 1979), along the lines presented in Section 1. Direct observational constraints on the shock amplitudes, the necessary ingredient for these studies, have been obtained by Hinkle (1978; Hinkle & Barnes 1979a,b; Hinkle et al 1982, 1984) for a number of Mira and SR variables using infrared CO observations. Typical shock amplitudes for Miras are 20–30 km s^{-1}, with the precise number depending on the (very uncertain) corrections made for integration

over the stellar disk. The smaller visual amplitude SR variables, in contrast, show shock amplitudes approximately half as large. This strongly supports the pulsation of the Miras being in the fundamental radial mode and leads to $T_{eff} > 3000$ K, in much better agreement with the excitation temperatures derived from the infrared CO lines (Lebzelter et al 1998).

Some investigators have suggested that some Miras pulsate in the fundamental mode while others are pulsating in an overtone (e.g. Van Leeuwen et al 1997). However, the homogeneity of shock amplitudes, the characteristic presence of emission lines during part of the cycle, and the tight P-L relation all argue strongly against the Mira class including variables pulsating in more than one mode. The light curve shapes of most Miras are also asymmetric, with the rapid rise that is characteristic of fundamental mode pulsation in other classes of stars and consistent with the appearance of fundamental mode models (but not with overtone models) by Bowen (1988, 1990).

Parallel sequences in L versus P would be expected if there are stars with otherwise similar properties pulsating in different modes. Such sequences have been identified in the LMC by Wood & Sebo (1996) and confirmed by Barthes (1998), although their interpretations differed. The massive data collection from the MACHO project data base supports this result (Wood 1999), showing clearly separated sequences in L versus P. The assumption that the Mira sequence corresponds to fundamental mode pulsation assigns the smaller-amplitude SRa stars to first and second overtones, a result that is also consistent with their more nearly sinusoidal light curves.

2.5 Empirical Mass Loss Laws

In 1975, Reimers published a correlation between observed mass loss rates and the combination of parameters LR/M for an assortment of red giants and supergiants:

$$\dot{M}_R = \eta\, 4 \times 10^{-13} LR/M, \tag{5}$$

where L, R, and M are in solar units and $\dot{M}$ is in $M_{Sun}\,yr^{-1}$. This relation provided stellar evolution modelers with a tool for investigating mass loss effects on stellar evolution, which they were not slow to exploit. It soon became clear that Equation 5 overestimated the mass loss during some stages of evolution, and underestimated the rates relative to those found at the tip of the AGB; thus the variable parameter η was introduced to allow better matching between HR diagrams and models.

As noted in Section 1, $L_{wind} \sim \dot{M}\, v_{esc}{}^2$. If the efficiency of all winds is about the same, $L_{wind} \sim 10^{-6}\, L_*$, then we recover Reimers' relation for $\eta = 1$. However, it is certainly not obvious a priori that the efficiency should be the same, particularly when such a very small fraction of the total luminosity is involved. A very different interpretation of this observed correlation of mass loss rate with stellar parameters is described in Section 3.

With the advent of more and more sensitive methods for detecting mass loss, it has become apparent that there are many stars with $\dot{M} >$ or $\gg \dot{M}_R$, and there

are certainly stars with $\dot{M} <$ or $\ll \dot{M}_R$. This has motivated a number of attempts to refine the relation, with L, R, and/or M allowed to have arbitrary exponents or more complex functional forms fitted to more extensive mass loss data. Adding more parameters reduces the scatter, of course, but does not really address the underlying issues. Invoking a "superwind" phase (Iben & Renzini 1983) near the end of the AGB improved the evolutionary models' match to observations, at the expense of adding more tunable parameters. Wood & Cahn (1977) were the first to examine the pattern of AGB evolution with mass loss. Recent examples of detailed "synthetic evolution" patterns for the AGB using a variety of mass loss laws may be found in Blöcker (1995) and Groenewegen & De Jong (1994). The result may be made to fit observable nearby populations almost arbitrarily well, but has little or no power to extend to situations not readily observable, such as young, low-metallicity stellar populations.

A different approach was taken by Vassiliadis & Wood (1993) for modeling terminal AGB evolution. They found a relationship between $\dot{M}$ and the pulsation period, P, an easily observed quantity that is also easily calculated for a given stellar model. Their fit captures the precipitous steepness of the mass loss law seen in the Bowen models, but not the spread for different masses. At a given P there is a wide range in $\dot{M}$, presumably because the stars with one P do not all have the same L, R, and M. The variation or scatter is entirely in the $\dot{M}$ axis, since P is easily observed to high accuracy. Thus, Vassiliadis & Wood's relation misses a substantial fraction of the mass dependence of $\dot{M}$, limiting its usefulness for population studies. This relation also does not include any basis for extension to metallicities other than the one used for the calibration.

Baud & Habing (1983) proposed a modification to Reimers' formula involving the envelope mass:

$$\dot{M} = (4 \times 10^{-3})(M_{env,o}/M_{env})LR/M \tag{6}$$

where $M_{env,o}$ is the mass of the envelope at the start of the AGB. This introduces a rapid "superwind" evaporation of the last portion of the stellar envelope.

In Figure 6, four empirical mass loss relations are compared. A set of evolutionary tracks (from Iben 1984; Equation 7, Section III) and the definition of effective temperature have been used to reduce the parameters to a single one, L, for each mass and composition. L thus represents the position along the AGB or, approximately, the time elapsed on the AGB (since $\Delta t \propto \Delta \log L$). Vassiliadis & Wood's relation gives a narrower range of L, over which the envelope mass would be lost, than does the Reimers' relation, and this would still be true with larger or smaller η (since η does not change the slope of log $\dot{M}$ versus log L). Baud & Habing's relation deviates from Reimers' relation only at the highest mass loss rates. The relation by Nieuwenhuijzen & De Jager (1990) was derived from observations of luminous supergiants, and as a result predicts large mass loss rates only at large L. The panels in this figure may be directly compared with Figure 4 at the end of Section 1, where mass loss laws from theoretical computations were displayed.

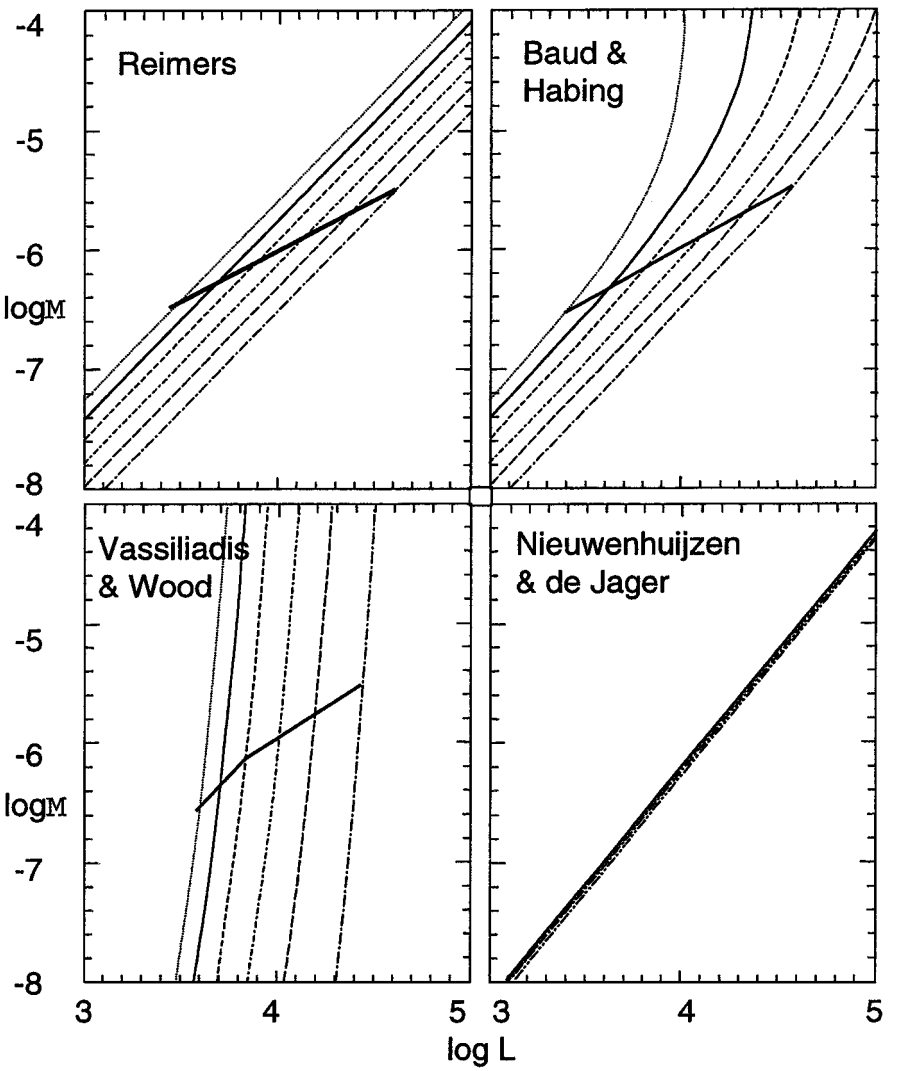

Figure 6 Mass loss rates versus luminosity computed from four empirical relations (Reimers 1975, Baud and Habing 1983, Vassiliadis & Wood 1993, Nieuwenhuijzen & De Jager 1990) in the same way as for the theoretical relations of Figure 4. In the first three panels, $M_{Sun} = 0.1$, 1, 1.4, 2, 2.8, and 4 are shown, with the heaviest line for $M_{Sun} = 1\ M_{Sun}$; in the fourth panel, $M = 5.6$, and 8 M_{Sun} have been added, since this formula was derived for more luminous and more massive stars. Across the first three panels, the location of the "cliff" or critical mass loss rate is shown. The law derived from more luminous stars predicts a higher terminal luminosity, as would be expected from the interpretation given in Section 3.

3. EVOLUTION WITH MASS LOSS

In the introduction the current state of evolutionary modeling with and without mass loss was reviewed. In this section an alternative approach to incorporating observational constraints on mass loss into theoretical modeling is demonstrated for the case of evolution on the asymptotic giant branch, building on the material presented in the preceding sections.

3.1 The Use and Interpretation of Empirical Relationships

The approach that has been most widely used to incorporate mass loss into stellar evolution calculations has been to look for a functional dependence of the mass loss rate on stellar parameters; to use this dependence in evolutionary calculations; and, if necessary, to adjust the mass loss law and repeat the process. At the end of Sections 1 and 2, a variety of mass loss laws derived from theoretical and observational studies were compared in terms of their predictions for the relation between L and $\dot{M}$.

There is a developing consensus, among those doing detailed modeling for the mass loss at the end of the AGB phase, that this mass loss depends much more steeply on stellar parameters than was evident from the first empirical relations (Bowen & Willson 1991, Höfner & Dorfi 1997, 1998a,b, Schröder et al 1999). This leads to a picture of the final evolution where the mass remains effectively constant until the star reaches a "cliff," the locus where $d \log M/dt \sim d \log L/dt$. With a small evolution in the stellar parameters—L, T_{eff}, and M—the mass loss rate rises precipitously and the star loses its envelope in a nearly exponential process. This is illustrated in Figure 7, which is based on Bowen's 1995 grid of models (also Bowen 2000, in preparation).

With a pattern such as the one in Figure 7, there will be very strong selection effects concerning stars for which mass loss will be measurable. Those not yet near the cliff will have low mass loss rates, while those beyond it will be short-lived (and probably also well obscured). Thus, we would expect a selection of stars with observed mass loss rates (such as Reimers used to establish a relation between mass loss rates and LR/M) to feature mainly stars within 1 dex in $\dot{M}$ of the cliff. Those lines (for the cliff models of Figure 7) are plotted in Figure 8, where clearly the Reimers relation is very well reproduced. Thus, the empirical mass loss laws tell us the parameters of stars that are losing mass, and not the dependence of mass loss rates on the parameters of any individual star. Two stars with the same period will have nearly the same mean density and, given that the masses are not too different, similar radii. The Miras and OH-IR stars also do not differ hugely in L and T_{eff} at a given P. However, the mass loss rates observed for Miras at a given P cover a range of several dex, illustrating again that the mass loss rates are very sensitive to stellar parameters.

In Figure 9 the "cliff" locations for populations with five different metallicities are plotted. To produce this figure, Bowen computed grids of dozens of

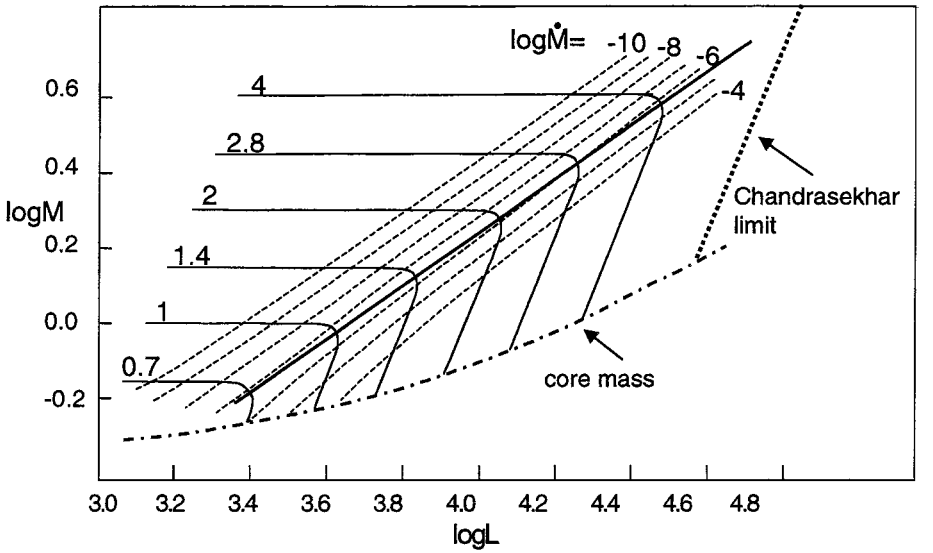

Figure 7 Evolution in mass and luminosity for solar composition stars. Contours of constant mass loss rate are indicated; the fact that these are very close together makes the "corner" on the cliff sharp. A star evolves at approximately constant mass until it is near the cliff; it leaves the cliff on an asymptote to a line of constant core mass. (Figure courtesy of GH Bowen.)

atmosphere-plus-wind models for each metallicity, using the Iben (1984) relation,

$$R = 312(L/10^4)^{0.68}(1.175/M)0^{32S}(Z/0.001)^{0.088}\alpha^{-0.52} \quad (7)$$

(where $S = 0$ for $M < 1.175$ and $S = 1$ for $M \geq 1.175$) to constrain the models to lie along a consistent set of evolutionary tracks. (A similar pattern would emerge for a different choice of evolutionary tracks or of α, the ratio of mixing length to scale height, as long as the following still holds true: More massive stars are hotter at a given L. Lower metallicity stars are hotter at a given L. As a star evolves to higher L, its T_{eff} decreases slowly.)

Figure 9 suggests that in young, low-metallicity populations compared with Pop. I we should expect higher-mass white dwarfs, more supernovae with the extras being of Type 1.5, less mass returned to the ISM, and most of the mass that is lost coming from a higher L stage on the AGB. This is the kind of information that is essential in order to improve our understanding of the early chemical evolution of the Milky Way. These results are also needed for modeling the appearance and chemical evolution of low-metallicity galaxies, including some starburst systems and most of the sources seen at high redshift.

The stars we classify as Miras are those that lie along the "cliff" line in Figure 7. From the models we can compute the periods (given the mode) and the luminosities of these cliff stars. In Figure 5, the resulting P-L relation (for fundamental mode)

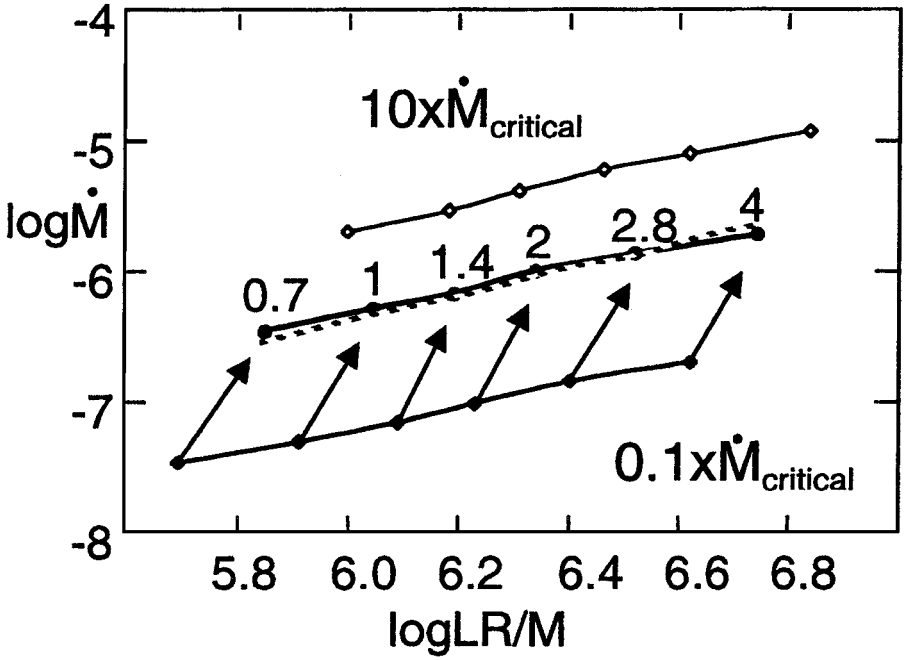

Figure 8 Mass loss rate versus LR/M for the "cliff" stars and mass loss rates 1/10, 10 times the "cliff" rates. Reimers (1975) relation is seen to coincide almost exactly with the "cliff" position. Thus Reimers' relation tells us the properties of stars when they are losing mass, not how any one star loses mass over time.

was superimposed on the observed P-L relation for LMC Miras. No parameter adjustment was made to achieve this fit.

Several conclusions that can be drawn from the above stand in contrast with current practices in putting mass loss into evolutionary and stellar population models. First, the mass loss along the AGB is abrupt, not gradual. Second, mass loss prior to the AGB is not enough to reduce all Miras to $\sim$1 solar mass. Third, the empirical P-L relation, having been confirmed by theory, may be relied on as a distance indicator. Fourth, empirical relations give us the properties of stars that are near a critical stage of losing mass, rather than telling us how to incorporate mass loss into evolutionary calculations. Fifth, because the significant mass loss is limited to a short duration near the end of the evolution on the AGB, tabulated evolutionary models that incorporate Reimers-type mass loss laws are less useful than models without any mass loss at all.

Three very significant problems remain in the study of mass loss from evolved red giants. The first has to do with the transformation of some stars into carbon stars. Figure 9 shows where stars reach critical mass loss rates if they remain spectral type M stars, i.e. as long as the carbon abundance in their envelopes stays less than the oxygen abundance. For a star that becomes a carbon star, some of

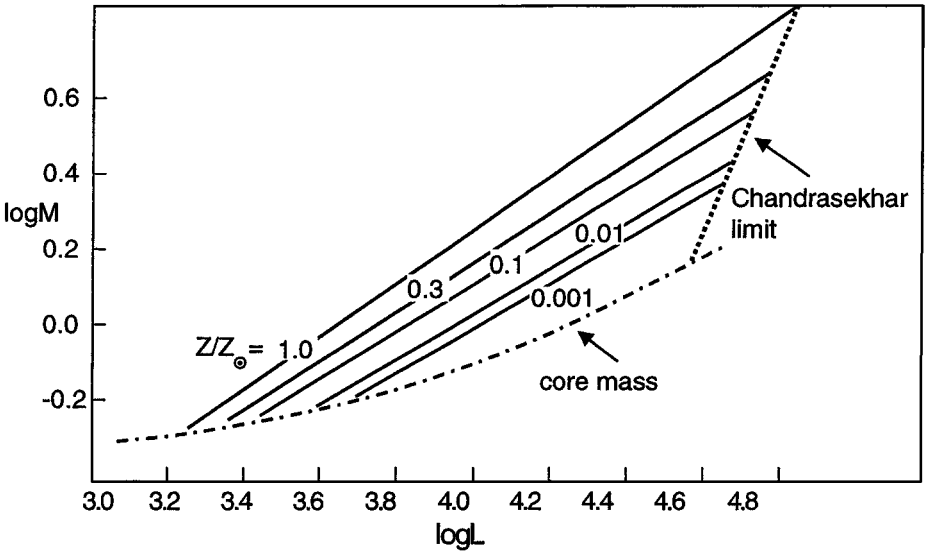

Figure 9 Cliff lines for five metallicities: 1, 0.3, 0.1, 0.01, and 0.001 times solar, with the Paczynski (1970) core mass relation also shown as a rough guide to the core mass. The shift of the cliff to higher L for lower Z comes primarily from the smaller radii at a given L of the lower-metallicity stars; the effects of dust are important only for the largest metallicities and the larger masses (Bowen 2000, in preparation). (Figure courtesy of GH Bowen.)

the relations that went into defining the cliff may need to be changed. The transition to C > O may change the relations among T_{eff} and M and L as the opacity changes in the outer envelope of the star. It greatly changes the character of the dust that plays a role in driving mass loss from some of these stars. Carbon star variables are not often classified as Mira variables, because they generally show smaller visual amplitudes, for reasons that are not yet clear. Unfortunately, in addition to the preceding uncertainties regarding the mass loss from carbon stars, we also do not yet have a reliable means of predicting which stars will become carbon stars and when, because this process involves mixing from the nuclear burning regions presumably associated with the helium shell flashes (Iben & Renzini 1983). Further, mass loss affects whether model stars become carbon stars (Frost et al 1998a,b; Lattanzio 1998). Thus we don't even know yet where to draw the gaps in the cliff lines in Figure 9, much less where to put the C^* cliffs. Finally, carbon star mass loss models fully compatible with available oxygen-rich star models do not yet exist, although progress is continuing toward that goal. However, all is not lost. There are observational hints that the cliffs may not be very far apart: The P-L relation for Magellanic Cloud carbon star variables is not very different from the P-L relation for oxygen-rich Miras (Hughes & Wood 1990). Also, the observed mass loss rates of carbon stars in the LMC fall in about the same region of the $\dot{M}$ versus log L plots that we expect the oxygen-rich stars to occupy (Van Loon et al 1997), also hinting that the cliffs may not be too far separated.

The second largely unsolved problem is understanding the modulation of the mass loss that takes place over the shell flash cycle. There is interest in this problem, and attempts have been made to solve it using a variety of tools. While it is straightforward to derive a mass loss rate formula from constant L, M, R models and then apply this formula to the time-variable L and R of a shell flash, this probably does not give a very good picture of the true event. Typically, the mass loss models need to be gradually brought to full amplitude or to a new period of oscillation; if this is not done, transient mass loss events develop (Hill & Willson 1979, Bowen 1988). Such transient events are likely to occur in real stars as well, and will require linked evolutionary and pulsation models.

The third unsolved problem is that of the mass loss that occurs at or near the tip of the red giant branch. Models for the evolution of low-mass red giants prior to the He core flash do not make it into the heavy mass loss region that the stars reach on the AGB. Is there mass loss associated with the core flash event? In contrast with earlier work by Schwarzschild and Härm (1962, Härm & Schwarzschild 1966) and Tomasko (1970) arguing that the main event is slow enough to avoid becoming hydrodynamic (although they didn't rule out some surface hydrodynamic effects), Cole and Deupree (1981) found that hydrodynamic loss of some of the envelope mass in response to a core flash is possible. Models are not yet to the state of being able to predict which stars will lose how much mass during a helium core flash, however. From the observational side, the distribution of stars along the horizontal branch constrains that mass loss for low-metallicity stars below about 1 solar mass; for these, one to several tenths of a solar mass of material must come off at that time. The Mira period-luminosity relation with the interpretation given above suggests that not very much mass is removed during the helium core flash for 1–3 M_{Sun} stars. For stars above 2 or 3 M_{Sun} there is no core flash (Sweigert & Gross 1978), so we have no reason to expect higher-mass stars to have significant mass loss at the end of the RGB.

In this section, I have focused on the mass loss that occurs near the end of the AGB for intermediate-mass stars. Apart from hints of some mass loss at the core flash, this is the only stage of evolution for stars less than 9 solar masses where we have clear evidence for mass loss sufficient to alter the fate of the star. Are there other stages of evolution where mass loss is important? I have not discussed pre-main-sequence stages, where there are certainly outflows, because these may originate from circumstellar disks more than from the star (Shu et al 1994a,b, 1995; Najita & Shu 1994, Ostriker & Shu 1995). Nor have I mentioned mass loss on the main sequence, although (given the long lifetimes of main sequence stars) such mass loss could occur without being easily detected (Willson et al 1987). Willson & Bowen (1984b) suggested that mass loss associated with pulsation might play a role in reducing evolutionary masses of Cepheids, since these were in conflict with their pulsation masses. Theoretical calculations confirmed that mass loss occurring during the Cepheid stage would work to reduce the evolutionary masses (Brunish & Willson 1987, 1989); however, new opacities have improved the agreement between the evolutionary and pulsation masses, so Cepheid-stage mass loss may not be required (Andreasen 1988). Willson & Bowen (1984b) also

suggested that pulsation-related mass loss from the RR Lyrae stars could send them off to the blue horizontal branch instead of up the AGB; theoretical models by Koopmann et al (1994) explored this hypothesis but found that it would not lead to the desired dispersion in color for any rates below 10^{-9} M_{Sun} yr^{-1}, and that higher mass loss rates would create other problems. Mullan (1996) derived high mass loss rates (given the evolutionary timescale) for cool dwarfs, but this result has also been questioned (Lim & White 1996, Van Den Oord & Doyle 1997).

At present the evidence is clear that mass loss at the end of the AGB is both measurable and important. There is no evidence that this is true for any other stage of evolution of stars below 9 M_{Sun}. Therefore, by studying the mass loss on the AGB we may derive most or all of what we need to know to incorporate mass loss into stellar evolution calculations for populations with ages between 10^8 and 10^{10} years.

SUMMARY/CONCLUSIONS

Stars with initial masses between about 1 and 9 solar masses that end up as white dwarf stars must lose a substantial fraction of their mass before they leave the asymptotic giant branch. Observational and theoretical studies over the past three decades have revealed that most of this mass loss occurs near the end of the AGB lifetime. Theoretical studies reveal that the dependence of the mass loss rate on stellar parameters is very steep. Observed correlations between mass loss rates and stellar parameters show much less sensitivity. The resolution of this apparent paradox lies in recognizing that where the mass loss varies over many orders of magnitude, observational selection effects will pick out stars whose mass loss rates are near the maximum value sustainable by the star.

Empirical mass loss laws cannot be derived unless the stellar parameters are well determined. For the Miras, heavily mass-losing stars at the tip of the AGB, the period-luminosity law derived from observations in the Magellanic Clouds appears to be quite good. Hipparcos data show considerably more scatter, possibly because of difficulties associated with measuring stars whose angular diameters equal or exceed the expected parallax. Angular diameters for Miras appear to be much less reliable that we would expect, likely because there is more contribution from scattering in the circumstellar envelope than has been included in any of the models. Progenitor masses deduced from kinematics of Miras are consistent with masses deduced from a theoretical fit to the P-L relation, suggesting that relatively little mass loss actually occurs before the end of the AGB.

Interpretation of observations of winds in cool stars has often been carried out using variations on the classical theory of stationary winds. However, the family of possible solutions for cool stars may be considerably more varied, since time variability (waves, noise from near-surface convection zones, pulsation), departures from spherical symmetry (bipolar flows and diverging coronal holes), and the effects of radiation pressure on (sometimes patchy) dust all play a role. To further

complicate the observational side, different methods sample different distances from the star, and thus different times, with evidence for time-variable outflow on scales of decades to 10^5 years.

A framework has been developed for understanding AGB mass loss; there is now a good match between theoretical computations and observed patterns for the AGB. This will allow the extrapolation of relations for terminal AGB luminosity and remnant masses to populations that are difficult to study directly. Young, low-metallicity populations are expected to have less mass loss, and thus higher mass remnants and more supernovae of Type 1.5, as a result of the dual effects of smaller radii at a given L and less dust.

ACKNOWLEDGMENTS

The author would like to thank Jeffrey S. Willson for exorcising the bibliographic demon. Support for dynamical atmosphere and mass loss studies from NASA over the past two decades is also gratefully acknowledged, including current grant NAG58465. This paper would have been quite different without the contributions of G. H. Bowen to research in this field; his generous contribution of several key figures is also acknowledged.

LITERATURE CITED

Andreasen GK. 1988. *Astron. Astrophys.* 201: 72–79

Arndt TU, Fleischer AJ, Sedlmayr E. 1997. *Astron. Astrophys.* 327:614–19

Asplund M. 1995. *Astron. Astrophys.* 294: 763–72

Barthes D. 1998. *Astron. Astrophys.* 333: 647–57

Baud B, Habing HJ. 1983. *Astron. Astrophys.* 127:73–83

Becker SA, Iben I, Jr. 1979. *Ap. J.* 232:831–53

Bedijn PJ. 1987. *Astron. Astrophys.* 186: 136–52

Berruyer N. 1991. *Astron. Astrophys.* 249: 181–91

Bessell MS, Brett JM, Wood PR, Scholz M. 1989. *Astron. Astrophys.* 213:209–25

Bester M, Danchi WC, Degiacomi CG, Townes CH, Geballe TR. 1991. *Ap. J.* 367:L27

Blöcker T. 1995. *Astron. Astrophys.* 297:727

Bonneau D, Foy R, Blazit A, Labeyrie A. 1982. *Astron. Astrophys.* 106:235

Bowen GH. 1988. *Ap. J.* 329:299–317

Bowen GH. 1990. In *Numerical Modeling of Nonlinear Stellar Pulsations. Problems and Prospects*, ed. JR Buchler. Dordrecht/ Boston:Kluwer. 155 pp.

Bowen GH, Willson LA. 1991. *Ap. J.* 375:L53–56

Bowers PF, Kerr FJ. 1977. *Astron. Astrophys.* 57:115–23

Boyle RP, Aspin C, McLean IS, Coyne GV. 1986. *Astron. Astrophys.* 164:310–20

Brunish WM, Willson LA. 1987. In *Stellar Pulsation*, ed. AN Cox, WM Sparks, SG Starrfield, p. 27. Berlin/New York: Springer-Verlag

Brunish WM, Willson LA. 1989. *The Use of Pulsating Stars in Fundamental Problems of Astronomy*, ed. EG Schmidt. Cambridge, UK: Cambridge Univ. Press. 252 pp.

Cadwell BJ, Wang H, Feigelson ED, Frenklach M. 1994. *Ap. J.* 429:285–99

Chamberlain JW. 1960. *Ap. J.* 131:47

Chamberlain JW. 1961. *Ap. J.* 133:675
Chamberlain JW. 1963. *Planet. Space Sci.* 11:901–60
Chan SJ, Kwok S. 1988. *Ap. J.* 334:362–96
Chiosi C, Bertelli G, Bressan A. 1992. *Annu. Rev. Astron. Astrophys.* 30:235–85
Chiosi C, Maeder A. 1986. *Annu. Rev. Astron. Astrophys.* 24:329–75
Clayton ML, Feast MW. 1969. *MNRAS* 146:411
Codina-Landaberry SJ, Magalhaes AM. 1980. *Astron. J.* 85:875–81
Cole PW, Deupree RG. 1981. *Ap. J.* 247: 607–11.
Cox JP, Giuli RT. 1968. *Principles of Stellar Structure*. New York: Gordon & Breach. 1327 pp.
Coyne GV, Magalhaes AM. 1977. *Astron. J.* 82:908–15
Coyne GV, Magalhaes AM. 1979. *Astron. J.* 84:1200–10
Cranmer SR, Field GB, Kohl JL. 1999. *Ap. J.* 518:937–47
Cuntz M. 1989. *PASP* 101:560
Cuntz M, Ulmschneider P, Musielak ZE. 1998. *Ap. J.* 493:L117
Danchi WC, Bester M. 1995. *Astrophys. Space Sci.* 224:339–52
Danchi WC, Bester M, Degiacomi CG, Greenhill LJ, Townes CH. 1994. *Astron. J.* 107:1469–513
Danchi WC, Bester M, Greenhill LJ, Degiacomi CG, Geis N, et al. 1995. *Astrophys. Space Sci.* 224:447–48
Donn B. 1978. In *Protostars and Planets*, ed. T Gehrels, pp. 100–33. Tucson: University of Arizona Press
Donn B, Nuth JA. 1985. *Ap. J.* 288:187–90
Draine BT. 1979. *Astrophys. Space Sci.* 65: 313–35
Draine BT. 1981. In *Physical Process in Red Giants*, eds. I Iben & A Renzini, pp. 317–33. Astrophysics and Space Science Library. Dordrecht/Boston/London: Reidel
Draine BT, Lee HM. 1984. *Ap. J.* 285:89–108
Draine BT, Lee HM. 1987. *Ap. J.* 318:485; erratum *Ap. J. Suppl.* 64:505
Draine BT, McKee CF. 1993. *Annu. Rev. Astron. Astrophys.* 31:373–432
Draine BT, Salpeter EE. 1979. *Ap. J.* 231:438–55
Drake SA, Linsky JL, Elitzur M. 1987. *Astron. J.* 94:1280–290
Drake SA, Linsky JL, Judge PG, Elitzur M. 1991. *Astron. J.* 101:230–36
Dupree AK. 1986. *Annu. Rev. Astron. Astrophys.* 24:377–420
Dyck M. 1987. See Kwok & Pottasch 1987, pp. 19–32
Elitzur M. 1992. *Annu. Rev. Astron. Astrophys.* 30:75–112
Elitzur M, Brown JA, Johnson HR. 1989. *Ap. J.* 341:L95–98
Feast MW, Glass IS, Whitelock PA, Catchpole RM. 1989. *MNRAS* 241:375–92
Fox MW, Wood PR. 1985. *Ap. J.* 297:455–75
Frost CA, Cannon RC, Lattanzio JC, Wood PR, Forestini M. 1998a. *Astron. Astrophys.* 332:L17–20
Frost CA, Lattanzio JC, Wood PR. 998b. *Ap. J.* 500:355
Gail HP, Sedlmayr E. 1987a. *Astron. Astrophys.* 171:197–204
Gail HP, Sedlmayr E. 1987b. *Astron. Astrophys.* 177:186–92
Gilman RC. 1969. *Ap. J.* 155:L185
Gilman RC. 1972. *Ap. J.* 178:423–26
Gilman RC. 1973. *MNRAS* 161:3P
Gilman RC. 1974. *Ap. J. Suppl.* 28:397
Glass IS, Catchpole RM, Feast MW, Whitelock PA, Reid IN. 1987. See Kwok & Pottasch 1987, pp. 51–54
Goldreich P, Scoville N. 1976. *Ap. J.* 205:144–54
Gray MD, Humphreys EML, Yates JA. 1999. *MNRAS* 304:906–24
Groenewegen MAT, De Jong T. 1994. *Astron. Astrophys.* 288:782–90
Guilain C, Mauron N. 1996. *Astron. Astrophys.* 314:585–93
Gustafsson B, Eriksson K, Kiselman D, Olander N, Olofsson H. 1997. *Astron. Astrophys.* 318:535–42
Hammer R. 1982. *Ap. J.* 259:767–91

Haniff CA, Scholz M, Tuthill PG. 1995. *MNRAS* 276:640
Härm R, Schwarzschild M. 1966. *Ap. J.* 145:496–504
Hartmann L, Macgregor KB. 1980. *Ap. J.* 242:260–82
Hashimoto O, Izumiura H, Kester DJM, Bontekoe TR. 1998. *Astron. Astrophys.* 329:213–18
Hashimoto O, Nakada Y, Onaka T, Kamijo F, Tanabe T. 1990. *Astron. Astrophys.* 227:465–72
Herpin F, Baudry A, Alcolea J, Cernicharo J. 1998. *Astron. Astrophys.* 334:1037–46
Hill SJ, Willson LA. 1979. *Ap. J.* 229:1029–45
Hinkle KH. 1978. *Ap. J.* 220:210–28
Hinkle KH. 1995. In *ASP Conf. Ser. 83, IAU Colloq. 155: Astrophysical Applications of Stellar Pulsation*, p. 399
Hinkle KH, Barnes TG. 1979a. *Ap. J.* 227:923–34
Hinkle KH, Barnes TG. 1979b. *Ap. J.* 234:548–55
Hinkle KH, Hall DNB, Ridgway ST. 1982. *Ap. J.* 252:697–714
Hinkle KH, Scharlach WWG, Hall DNB. 1984. *Ap. J. Suppl.* 56:1–17
Höfner S, Dorfi EA. 1992. *Astron. Astrophys.* 265:207–15
Höfner S, Dorfi EA. 1997. *Astron. Astrophys.* 319:648
Höfner S, Jørgensen UG, Loidl R. 1998a. *Astrophys. Space Sci.* 255:281–87
Höfner S, Jørgensen UG, Loidl R, Aringer B. 1998b. *Astron. Astrophys.* 340:497–507
Holm AV, Doherty LR. 1988. *Ap. J.* 328:726–33
Holzer TE. 1977. *J. Geophys. Res.* 82:23–35
Holzer TE, Axford WI. 1970. *Annu. Rev. Astron. Astrophys.* 8:31
Holzer TE, MacGregor KB. 1985. See Morris & Zuckerman 1985, p. 299
Hron J, Loidl R, Höfner S, Jørgensen UG, Aringer B, Kerschbaum F. 1998. *Astron. Astrophys.* 335:L69–72
Hughes SMG, Wood PR. 1990. *Astron. J.* 99:784–816
Humphreys EML, Gray MD, Field D, Yates JA, Bowen G. 1997a. *Astrophys. Space Sci.* 251:215–18
Humphreys EML, Gray MD, Yates JA, Field D. 1997b. *MNRAS* 287:663–70
Iben I, Jr. 1974. *Annu. Rev. Astron. Astrophys.* 12:215–56
Iben I, Jr. 1984. *Ap. J.* 277:333–54
Iben I, Jr, Renzini A, eds. 1981. *Physical Processes in Red Giants*. Dordrecht/Boston/Lancaster: Reidel. 488 pp.
Iben I, Jr, Renzini A. 1983. *Annu. Rev. Astron. Astrophys.* 21:271–342
Jones TJ, Bryja CO, Gehrz RD, Harrison TE, Johnson JJ, et al. 1990. *Ap. J. Suppl.* 74:785–817
Jørgensen UG, Johnson HR. 1992. *Astron. Astrophys.* 265:168–76
Jorissen A, Knapp GR. 1998. *Astron. Astrophys.* 129:363–98
Karovska M, Nisenson P, Papaliolios C, Boyle RP. 1991. *Ap. J.* 374:L51–54
Kerschbaum F, Hron J. 1996. *Astron. Astrophys.* 308:489–96
Knapp GR. 1986. *Ap. J.* 311:731–41
Knapp GR. 1991. In *ASP Conf. Ser. 20: Frontiers of Stellar Evolution*, pp. 229–63
Knapp GR, Bowers PF, Young K, Phillips TG. 1995. *Ap. J.* 455:293
Koopmann RA, Lee Y-W, Demarque P, Howard JM. 1994. *Ap. J.* 423:380–85
Krueger D, Sedlmayr E. 1997. *Astron. Astrophys.* 321:557–67
Kruszewski A, Gehrels T, Serkowski K. 1968. *Astron. J.* 73:677
Kwok S. 1975. *Ap. J.* 198:583–91
Kwok S. 1993. *Annu. Rev. Astron. Astrophys.* 31:63–92
Kwok S, Pottasch SR. 1987. *Late Stages of Stellar Evolution*. Dordrecht/Boston/Lancaster: Reidel. 426 pp.
Lamers HJGLM, Cassinelli IP. 1996. In *ASP Conf. Ser. 98, From Stars to Galaxies: the Impact of Stellar Physics on Galaxy Evolution*, p. 162
Lamers HJGLM, Cassinelli JP. 1999. *Introduction to Stellar Winds*. Cambridge, UK: Cambridge Univ. Press. 438 pp.

Lattanzi MG, Munari U, Whitelock PA, Feast MW. 1997. *Ap. J.* 485:328
Lattanzio JC. 1998. In *Stellar Evolution, Stellar Explosions and Galactic Chemical Evolution*, ed. A Mezzacappa, p. 299. Institute of Physics Publishing
Le Bertre T, Le Bertre A, Waelkens C, eds. 1999. *191 Asymptotic Giant Branch Stars.*
Lebzelter T, Hinkle KH, Hron J. 1998. *Astron. J.* 116:2520–29
Lepine JRD, Ortiz R, Epchtein N. 1995. *Astron. Astrophys.* 299:453
Lim J, White SM. 1996. *Ap. J.* 462:L91
Little-Marenin IR, Sahai R, Wannier PG, Benson PJ, Gaylard M, Omont A. 1994. *Astron. Astrophys.* 281:451–59
Loidl RH, Höfner S. Jørgensen UG, Aringer B. 1999. *Astron. Astrophys.* 342:531–41
Maciel WJ. 1976. *Astron. Astrophys.* 48:27–31
Mastrodemos N, Morris M, Castor J. 1996. *Ap. J.* 468:851
McLean IS, Coyne GV. 1978. *Ap. J.* 226:L145–48
Monnier JD, Geballe TR, Danchi WC. 1998. *Ap. J.* 502:833
Moore RL, Hammer R, Musielak ZE, Suess ST, An CH. 1992. *Ap. J.* 397:L55–58
Morris M, Zuckerman B, eds. 1985. *Mass Loss from Red Giants*. Los Angeles: Reidel. 320 pp.
Motteran M. 1971. In *Colloquium on Supergiant Stars*, ed. M Hack. Trieste:Osservatorio astronomico di Trieste, 371 pp.
Mould J, Reid N. 1987. *Ap. J.* 321:156–61
Mullan DJ. 1996. In *ASP Conf. Ser. 109, Ninth Cambridge Workshop on Cool Stars, Stellar Systems, and the Sun*, p. 461
Najita JR, Shu FH. 1994. *Ap. J.* 429:808–25
Netzer N, Elitzur M. 1993. *Ap. J.* 410:701–13
Nieuwenhuijzen H, De Jager C. 1990. *Astron. Astrophys.* 231:134–36
Nuth JA, Donn B. 1981. *Ap. J.* 247:925–35
Nyman LA, Booth RS, Carlström U, Habing HJ, Heske A, et al. 1992. *Astron. Astrophys. Suppl.* 93:121–50
Olofsson H. 1996a. *Astrophys. Space Sci.* 245:169–200
Olofsson H. 1996b. In *Molecules in Astrophysics: Probes & Processes: IAU Symposium 178*, ed. EF van Dishoeck, p. 457
Olofsson H. 1997. *Astrophys. Space Sci.* 251:31–39
Olofsson H, Bergman P, Eriksson K, Gustafsson B. 1996. *Astron. Astrophys.* 311:587–615
Olofsson H, Bergman P, Lucas R, Eriksson K, Gustafsson B, Bieging JH. 1998. *Astron. Astrophys.* 330:L1–4
Olofsson H, Carlström U, Eriksson K, Gustafsson B. 1992. *Astron. Astrophys.* 253:L17–20
Olofsson H, Carlström U, Eriksson K, Gustafsson B, Willson LA. 1990. *Astron. Astrophys.* 230:L13–16
Ostlie DA, Cox AN. 1986. *Ap. J.* 311:864–72
Ostriker EC, Shu FH. 1995. *Ap. J.* 447:813
Paczynski B. 1970. *Acta Astron.* 20:47
Parker EN. 1960. *Ap. J.* 132:821
Parker EN. 1961. *Ap. J.* 134:20
Parker EN. 1963a. *Space Sci. Rev.* 4:666–708
Parker EN. 1963b. *Interplanetary Dynamical Processes*. New York: Interscience, 272 pp.
Parker EN. 1964a. *Ap. J.* 139:72
Parker EN. 1964b. *Ap. J.* 139:93
Parker EN. 1964c. *Ap. J.* 139:690
Parker EN. 1965. *Ap. J.* 141:1463
Parker EN. 1966. *Ap. J.* 143:32
Parker EN. 1969. *Sp. Sci. Rev.* 9:325–360
Parker EN. 1997. In *Cosmic Winds and the Heliosphere*, ed. JR Jokipii, CP Sonett, MS Giampapa, pp. 3–30. Tucson: Univ. Ariz. Press
Patzer ABC, Gauger A, Sedlmayr E. 1998. *Astron. Astrophys.* 337:847–58
Percy JR, Colivas T. 1999. *PASP* 111:94–97
Perrin G, Coudé du Foresto V, Ridgway ST, Mennesson B, Ruilier C, et al. 1999. *Astron. Astrophys.* 345:221–32
Pijpers FP, Habing HJ. 1989. *Astron. Astrophys.* 215:334–46
Pugach AF. 1977. *Inf. Bull. Var. Stars* 1277:1
Quirrenbach A, Mozurkewich D, Armstrong JT, Buscher DF, Hummel CA. 1993. *Ap. J.* 406:215–19
Rammacher W, Ulmschneider P. 1992. *Astron. Astrophys.* 253:586–600
Reid MJ, Menten KM. 1997. *Ap. J.* 476:327

Reimers D. 1975. In *Problems in Stellar Atmospheres and Envelopes*, ed. B Baschek, WH Kegel, G Traving, pp. 229–56. Berlin/New York: Springer-Verlag
Ridgway ST, Wells DC, Joyce RR, Allen RG. 1979. *Astron. J.* 84:247–56
Sahai R, Liechti S. 1995. *Astron. Astrophys.* 293:198–207
Sahai R, Wannier PG. 1992. *Ap. J.* 394:320–39
Salpeter EE. 1974a. *Ap. J.* 193:579–84
Salpeter EE. 1974b. *Ap. J.* 193:585–92
Salpeter EE. 1977. *Annu. Rev. Astron. Astrophys.* 15:267–93
Schönberner D. 1983. *Ap. J.* 272:708–14
Scholz M, Takeda Y. 1987. *Astron. Astrophys.* 186:200–12
Schröder KP, Winters JM, Sedlmayr E. 1999. *Astron. Astrophys.* 349:898–906
Schwarzschild M, Härm R. 1962. *Ap. J.* 135:158–65
Shu F, Najita J, Ostriker E, Wilkin F, Ruden S, Lizano S. 1994a. *Ap. J.* 429:781–96
Shu FH, Najita J, Ruden SP, Lizano S. 1994b. *Ap. J.* 429:797–807M
Shu FH, Najita J, Ostriker EC, Shang H. 1995. *Ap. J.* 455:L155
Sopka RJ, Olofsson H, Johansson LEB, Nguyen-Rieu Q, Zuckerman B. 1989. *Astron. Astrophys.* 210:78–92
Spergel DN, Giuliani JL, Jr, Knapp GR. 1983. *Ap. J.* 275:330–41
Spitzer LJ. 1968. *Diffuse Matter in Space*. New York: Interscience Publishers. 262 pp.
Stephens JR. 1991. In *Proceedings of the International School of Physics "Enrico Fermi" Course CXI: Solid State Astrophysics*, ed. E Bussoletti and G Strazzulla, 391–402. Amsterdam/New York: Elsevier
Sterken C, Broens E, Koen C. 1999. *Astron. Astrophys.* 342:167–72
Sutmann G, Ulmschneider P. 1995. *Astron. Astrophys.* 294:241–51
Sweigart AV, Greggio L, Renzini A. 1990. *Ap. J.* 364:527–39
Sweigart AV, Gross PG. 1978. *Ap. J. Suppl.* 36:405–37
Tielens AGGM. 1983. *Ap. J.* 271:702–16
Tielens AGGM. 1998. *Ap. J.* 499:267
Tielens AGGM, McKee CF, Seab CG, Hollenbach DJ. 1994. *Ap. J.* 431:321–40
Tomasko MG. 1970. *Ap. J.* 162:125–38
Tsuji T. 1978. *Pub. Astron. Soc. J.* 30:435–54
Tuthill PG, Haniff CA, Baldwin JE. 1995. *MNRAS* 277:1541
Ulmschneider R, Schmitz F, Kalkofen W, Bohn HU. 1978. *Astron. Astrophys.* 70:487
Van Belle GT, Dyck HM, Benson JA, Lacasse MG. 1996. *Astron. J.* 112:2147
Van Belle GT, Dyck HM, Thompson RR, Benson JA, Kannappan SJ. 1997. *Astron. J.* 114:2150
Van Den Oord GHJ, Doyle JG. 1997. *Astron. Astrophys.* 319:578–88
Van Der Veen WECJ, Habing HJ. 1988. *Astron. Astrophys.* 194:125–34
Van Der Veen WECJ, Rugers M. 1989. *Astron. Astrophys.* 226:183–202
Van Langevelde HJ, Van Der Heiden R, Van Schooneveld C. 1990. *Astron. Astrophys.* 239:193–204
Van Leeuwen F, Feast MW, Whitelock PA, Yudin B. 1997. *MNRAS* 287:955–60
Van Loon JT, Groenewegen MAT, De Koter A, Trams NR, Waters LBFM, et al. 1999. *Astron. Astrophys.* 351:559–72
Vassiliadis E, Wood PR. 1992. *Proc. Astron. Soc. Austr.* 10:30–32
Vassiliadis E, Wood PR. 1993. *Ap. J.* 413:641–57
Wallerstein G, Knapp GR. 1998. *Annu. Rev. Astron. Astrophys.* 36:369–434
Walmsley CM, Chini R, Kreysa E, Steppe H, Forveille T, Omont A. 1991. *Astron. Astrophys.* 248:555–62
Wannier PG, Sahai R. 1986. *Ap. J.* 311:335–44
Wannier PG, Sahai R, Andersson BG, Johnson HR. 1990. *Ap. J.* 358:251–61
Weidemann V. 1990. *Annu. Rev. Astron. Astrophys.* 28:103–37
Weymann R. 1963. *Annu. Rev. Astron. Astrophys.* 1:97
Willson LA. 1999. In *Unsolved Problems in Stellar Evolution*, ed. M Livio, p. 227. Cambridge, UK: Cambridge Univ. Press

Willson LA, Bowen GH. 1984a. In *The Relationship Between Chromospheric/Coronal Heating and Mass Loss*, ed. R Stalio, J, Zirker, pp. 127–56. Triesta:NASA SP

Willson LA, Bowen GH. 1984b. *Nature* 312:429–31

Willson LA, Bowen GH. 1988. In *Polarized Radiation of Circumstellar Origin*, ed. G Coyne SJ, pp. 485–510. Castel Gandolfo:Univ. Ariz. Press

Willson LA, Bowen GH. 1988. In *Cyclical Variability in Stellar Winds*, Proceedings of the ESO Workshop held at Garching, Germany, 14–17 October 1997, ed. L Kaper, AW Fullerton, p. 294. Berlin/New York: Springer-Verlag

Willson LA, Bowen GH, Struck C. 1996. In *ASP Conf. Ser. 98, From Stars to Galaxies: The Impact of Stellar Physics on Galaxy Evolution*, p. 197

Willson LA, Bowen GH, Struck-Marcell C. 1987. *Comments Asrophys.* 12:17–34

Willson LA, Hill SJ. 1979. *Ap. J.* 228:854–69

Willson LA, Wallerstein G, Pilachowski CA. 1982. *MNRAS* 198:483–516

Windsteig W, Drofi EA, Hoefner S, Hron J, Kerschbaum F. 1997. *Arstron. Astrophys.* 324:617–23

Winters JM, Fleischer AJ, Le Bertre T, Sedlmayr E. 1997. *Astron. Astrophys.* 326:305–17

Withbroe GL. 1988. *Ap. J.* 325:442–67

Withbroe GL, Noyes RW. 1977. *Annu. Rev. Astron. Astrophys.* 15:363–87

Woitke P, Krueger D, Sedlmayr E. 1996. *Astron. Astrophys.* 311:927–44

Wolff MJ, Clayton GC, Gibson SJ. 1998. *Ap. J.* 503:815

Wood PR. 1974. *Ap. J.* 190:609–30

Wood PR. 1979. *Ap. J.* 227:220–31

Wood PR. 1990. In *ASP Conf. Ser. 11, Conformation Between Stellar Pulsation and Evolution*, pp. 355–63

Wood PR. 1998. *Astron. Astrophys.* 338:592–98

Wood PR. 1999. In *ASP Conf. Ser 191, Asymptotic Giant Branch Stars* ed. Bertre T, Lebre A, Waelkens C. p. 151

Wood PR, Cahn JH. 1977. *Ap. J.* 211:499–508

Wood PR, Sebo KM. 1996. *MNRAS* 282:958–64

Wood PR, Whiteoak JB, Hughes SMG, Besell MS, Gardner FF, Hyland AR. 1992. *Ap. J.* 397:552–69

Wood PR, Zarro DM. 1981. *Ap. J.* 247:247–56

Zuckerman B. 1980. *Annu. Rev. Astron. Astrophys.* 18:263–88